

QGP universality in a magnetic field?

Alex Buchel^{1,2,3} and Bruno Umbert^{1,3}

¹*Department of Applied Mathematics*

²*Department of Physics and Astronomy*

University of Western Ontario

London, Ontario N6A 5B7, Canada

³*Perimeter Institute for Theoretical Physics*

Waterloo, Ontario N2J 2W9, Canada

Abstract

We use top-down holographic models to study the thermal equation of state of strongly coupled quark-gluon plasma in external magnetic field. We identify different conformal and non-conformal theories within consistent truncations of $\mathcal{N} = 8$ gauged supergravity in five dimensions (including STU models, gauged $\mathcal{N} = 2^*$ theory) and show that the ratio of the transverse to the longitudinal pressure P_T/P_L as a function of T/\sqrt{B} can be collapsed to a 'universal' curve for a wide range of the adjoint hypermultiplet masses m . We stress that this does not imply any hidden universality in magnetoresponse, as other observables do not exhibit any universality. Instead, the observed collapse in P_T/P_L is simply due to a strong dependence of the equation of state on the (freely adjustable) renormalization scale: in other words, it is simply a fitting artifact. Remarkably, we do uncover a different universality in $\mathcal{N} = 2^*$ gauge theory in the external magnetic field: we show that magnetized $\mathcal{N} = 2^*$ plasma has a critical point at T_{crit}/\sqrt{B} which value varies by 2% (or less) as $m/\sqrt{B} \in [0, \infty)$. At criticality, and for large values of m/\sqrt{B} , the effective central charge of the theory scales as $\propto \sqrt{B}/m$.

April 3, 2020

Contents

1	Introduction and summary	2
2	Technical details	14
2.1	CFT_{diag}	15
2.2	CFT_{STU}	15
2.3	$n\text{CFT}_m$	20
2.3.1	$\text{CFT}_{PW,m=0}$	24
2.3.2	$\text{CFT}_{PW,m=\infty}$	25
A	Proof of $-P_L = \mathcal{E} - sT$ in holographic magnetized plasma	30
B	Conformal models in the limit $T/\sqrt{B} \gg 1$	31
B.1	CFT_{STU}	31
B.2	$\text{CFT}_{PW,m=0}$	35
B.3	$\text{CFT}_{PW,m=\infty}$	38
C	FT and TR in a $n\text{CFT}_m$ model	40

1 Introduction and summary

In [1] the authors used the recent lattice QCD equation of state (EOS) data in the presence of a background magnetic field [2, 3], and the holographic EOS results¹ for the strongly coupled $\mathcal{N} = 4$ $SU(N)$ maximally supersymmetric Yang-Mills (SYM) to argue for the universal magnetoresponse. While $\mathcal{N} = 4$ SYM is conformal, the scale invariance is explicitly broken by the background magnetic field B and its thermal equilibrium stress-energy tensor is logarithmically sensitive to the choice of the renormalization scale. It was shown in [1] that both the QCD and the $\mathcal{N} = 4$ data (with optimally adjusted renormalization scale) for the pressure anisotropy R ,

$$R \equiv \frac{P_T}{P_L}, \tag{1.1}$$

¹Studied for the first time in [4].

i.e., defined as a ratio of the transverse P_T to the longitudinal P_L pressure², collapse onto a single universal curve as a function of T/\sqrt{B} , at least for $T/\sqrt{B} \gtrsim 0.2$ or correspondingly for $R \gtrsim 0.5$, see Fig. 6 of [1]. The authors do mention that the ‘universality’ is somewhat fragile: besides the obvious fact that large- N $\mathcal{N} = 4$ SYM is not QCD (leading to inherent ambiguities as to how precisely one would match the renormalization schemes in both theories — hence the authors opted for the freely-adjustable renormalization scale in SYM), one observes the universality in R , but not in other thermodynamic quantities (*e.g.*, P_T/\mathcal{E} — the ratio of the transverse pressure to the energy density).

So, is there a universal magnetoresponse? In this paper we address this question in a controlled setting: specifically, we consider holographic models of gauge theory/string theory correspondence [5, 6] where all the four-dimensional strongly coupled gauge theories discussed have the same ultraviolet fixed point — $\mathcal{N} = 4$ SYM. We discuss two classes of theories:

- conformal gauge theories corresponding to different consistent truncations of $\mathcal{N} = 8$ gauged supergravity in five dimensions³ [7];
- non-conformal $\mathcal{N} = 2^*$ gauge theory ($\mathcal{N} = 4$ SYM with a mass term for the $\mathcal{N} = 2$ hypermultiplet) [7–9] (PW).

In the former case, the anisotropic thermal equilibrium states are characterized by the temperature T , the background magnetic field B and the renormalization scale μ ; in the latter case, we have additionally a hypermultiplet mass scale m .

Before we present results, we characterize more precisely the models studied.

- CFT_{diag} : $\mathcal{N} = 4$ SYM has a global $SU(4)$ R -symmetry. In this model magnetic field is turned on for the diagonal $U(1)$ of the R -symmetry. This is the model of [1], see also [4]. See section 2.1 for the technical details.
- CFT_{STU} : Holographic duals of $\mathcal{N} = 4$ SYM with $U(1)^3 \subset SU(4)$ global symmetry are known as STU-models [10, 11]. In this conformal theory the background magnetic field is turned on for one of the $U(1)$ ’s. This model is a consistent truncation of $\mathcal{N} = 8$ five-dimensional gauged supergravity with two scalar fields dual to two dimension $\Delta = 2$

²We take a constant magnetic field to be $\mathbf{B} = B\mathbf{e}_z$ so that P_T and P_L are correspondingly the $\langle T_{xx} \rangle = \langle T_{yy} \rangle$ and the $\langle T_{zz} \rangle$ components of the stress-energy tensor.

³In this class of theories there is a well motivated choice of the renormalization scale — namely, it is natural to have it be the same for all the theories in the class.

operators. As we show in section 2.2, in the presence of the background magnetic field these operators will develop thermal expectation values.

- $n\text{CFT}_m$: As we show in section 2.3, within consistent truncation of $\mathcal{N} = 8$ five-dimensional gauged supergravity presented in [7], it is possible to identify a holographic dual to $\mathcal{N} = 2^*$ gauge theory with a single $U(1)$ global symmetry. In this model the background magnetic field is turned on in this $U(1)$. The label $m \in (0, +\infty)$ denotes the hypermultiplet mass of the $\mathcal{N} = 2^*$ gauge theory.

- $\text{CFT}_{PW,m=0}$: This conformal gauge theory is a limiting case of the nonconformal $n\text{CFT}_m$ model:

$$\text{CFT}_{PW,m=0} = \lim_{m/\sqrt{B} \rightarrow 0} n\text{CFT}_m.$$

Its bulk gravitational dual contains two scalar fields dual to dimension $\Delta = 2$ and $\Delta = 3$ operators of the $\mathcal{N} = 2^*$ gauge theory. As we show in section 2.3.1, in the presence of the background magnetic field these operators will develop thermal expectation values.

- $\text{CFT}_{PW,m=\infty}$: This conformal gauge theory is a limiting case of the nonconformal $n\text{CFT}_m$ model:

$$\text{CFT}_{PW,m=\infty} = \lim_{m/\sqrt{B} \rightarrow \infty} n\text{CFT}_m.$$

Its holographic dual can be obtained from the $\mathcal{N} = 8$ five dimensional gauged supergravity of [7] using the "near horizon limit" of [12]⁴, followed by the uplift to six dimensions — the resulting holographic dual is Romans $F(4)$ gauged supergravity in six dimensions [15, 16]⁵. The six dimensional gravitational bulk contains a single scalar, dual to dimension $\Delta = 3$ operator of the effective CFT_5 . There is no conformal anomaly in odd dimensions. Furthermore, there is no invariant dimension-five operator that can be constructed only with the magnetic field strength — as a result, the anisotropic stress-energy tensor of $\text{CFT}_{PW,m=\infty}$ plasma is traceless, and is *free* from renormalization scheme ambiguities. Details on the $\text{CFT}_{PW,m=\infty}$ model are presented in section 2.3.2. The renormalization scheme-independence of $\text{CFT}_{PW,m=\infty}$ is a welcome feature: we will use the pressure anisotropy (1.1) of the theory as a benchmark to compare with the other conformal and non-conformal models.

And now the results. There is no universal magnetoresponse. Qualitatively, among conformal/non-conformal models we observe three different IR regimes (*i.e.*, when

⁴See appendix D of [13] for details of the isotropic (no magnetic field) thermal states of $\mathcal{N} = 2^*$ plasma in the limit $m/T \rightarrow \infty$. The first hint that $\mathcal{N} = 2^*$ plasma in the infinite mass limit is an effective five dimensional CFT appeared in [14].

⁵See [17] for a recent discussion.

T/\sqrt{B} is small):

- In CFT_{diag} it is possible to reach deep IR, *i.e.*, the $T/\sqrt{B} \rightarrow 0$ limit. For $T/\sqrt{B} \lesssim 0.1$ the thermodynamics is BTZ-like with the entropy density⁶ [4]

$$s \rightarrow \frac{N^2}{3} BT, \quad \text{as} \quad \frac{T}{\sqrt{B}} \rightarrow 0. \quad (1.2)$$

- Both in $\text{CFT}_{PW,m=0}$ and $\text{CFT}_{PW,m=\infty}$ (and in fact in all $n\text{CFT}_m$ models) there is a terminal critical temperature T_{crit} which separates thermodynamically stable and unstable phases of the anisotropic plasma. Remarkably, this T_{crit} is universally determined by the magnetic field B , (almost) independently⁷ of the mass parameter m of $n\text{CFT}_m$:

$$\begin{array}{ccccc} \text{CFT}_{PW,m=0} & \longrightarrow & n\text{CFT}_m & \longrightarrow & \text{CFT}_{PW,m=\infty} \\ \\ \frac{T_{crit}}{\sqrt{B}} : & 0.29823(5) & \longrightarrow & [0.29823(6), 0.30667(1)] & \longrightarrow & 0.30673(9) \\ \\ \frac{m}{\sqrt{2B}} : & 0 & \longrightarrow & [1/100, 10] & \longrightarrow & \infty, \end{array}$$

i.e., the variation of T_{crit}/\sqrt{B} with mass about its mean value is 2% or less, see Fig. 7 (left panel). We leave the extensive study of this critical point to future work, and only point out that the specific heat at constant B at criticality has a critical exponent⁸ $\alpha = \frac{1}{2}$:

$$c_B = -T \frac{\partial^2 \mathcal{F}}{(\partial T)^2} \Big|_B = \frac{\partial s}{\partial \ln T} \Big|_B \propto (T - T_{crit})^{-1/2}, \quad (1.3)$$

where \mathcal{F} is the free energy density, see Fig. 6.

- The CFT_{STU} model in the IR is different from the other ones. We obtained reliable numerical results in this model for $T/\sqrt{B} \gtrsim 0.06$: we neither observe the critical point as in the $\text{CFT}_{PW,m=0}$ and $\text{CFT}_{PW,m=\infty}$ models, nor the BTZ-like behavior (1.2) as in the CFT_{diag} model, see Fig. 3 (left panel).

In Fig. 1 we present the pressure anisotropy parameter R (1.1) for the conformal theories: CFT_{diag} (black curves), CFT_{STU} (blue curves), $\text{CFT}_{PW,m=0}$ (green curves)

⁶We independently reproduce this result.

⁷A very weak dependence on the mass parameter has been also observed for the equilibration rates in $\mathcal{N} = 2^*$ isotropic plasma in [18].

⁸The critical point with the same mean-field exponent α has been observed in isotropic thermodynamics of $\mathcal{N} = 2^*$ plasma with different masses for the bosonic and fermionic components of the hypermultiplet [19].

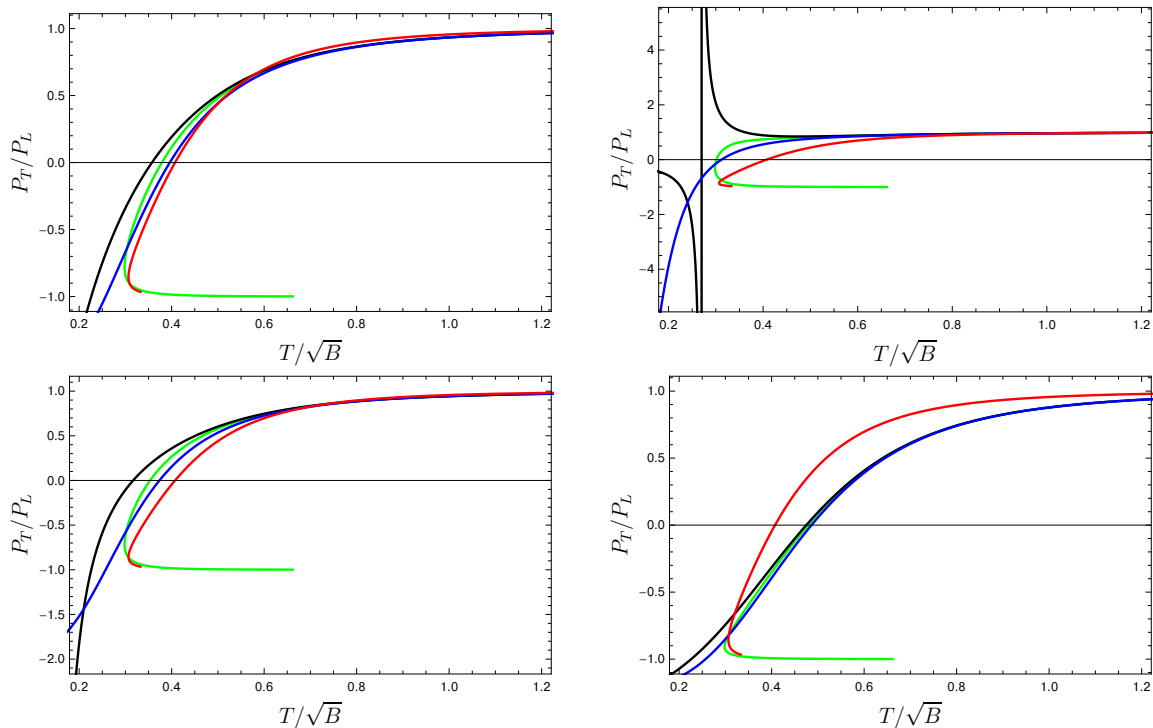


Figure 1: Anisotropy parameter $R = P_T/P_L$ for conformal models CFT_{diag} (black curves), CFT_{STU} (blue curves), $\text{CFT}_{PW,m=0}$ (green curves) and $\text{CFT}_{PW,m=\infty}$ (red curves) as a function of T/\sqrt{B} . $R_{\text{CFT}_{PW,m=\infty}}$ is renormalization scheme independent; for the other models there is a strong dependence on the renormalization scale $\delta = \ln \frac{B}{\mu^2}$: different panels represent different choices for δ ; all the models in the same panel have the same value of δ , leading to identical high-temperature asymptotics, $T/\sqrt{B} \gg 1$.

and $\text{CFT}_{PW,m=\infty}$ (red curves) as a function of⁹ T/\sqrt{B} . R is renormalization scheme independent in the $\text{CFT}_{PW,m=\infty}$ model, while in the former three conformal models it is sensitive to

$$\delta \equiv \ln \frac{B}{\mu^2}, \quad (1.4)$$

where μ is the renormalization scale. We performed high-temperature perturbative analysis, *i.e.*, as $T/\sqrt{B} \gg 1$, to ensure that the definition of δ is consistent across all the conformal models sensitive to it, see appendix B. In the { top left, top right, bottom left, bottom right } panel of Fig. 1 we set $\{\delta = 4, \delta = 2.5, \delta = 3.5, \delta = 7\}$ (correspondingly) for $R_{\text{CFT}_{diag}}$, $R_{\text{CFT}_{STU}}$ and $R_{\text{CFT}_{PW,m=0}}$ — notice that while all the

⁹We use the same normalization of the magnetic field in holographic models as in [1].

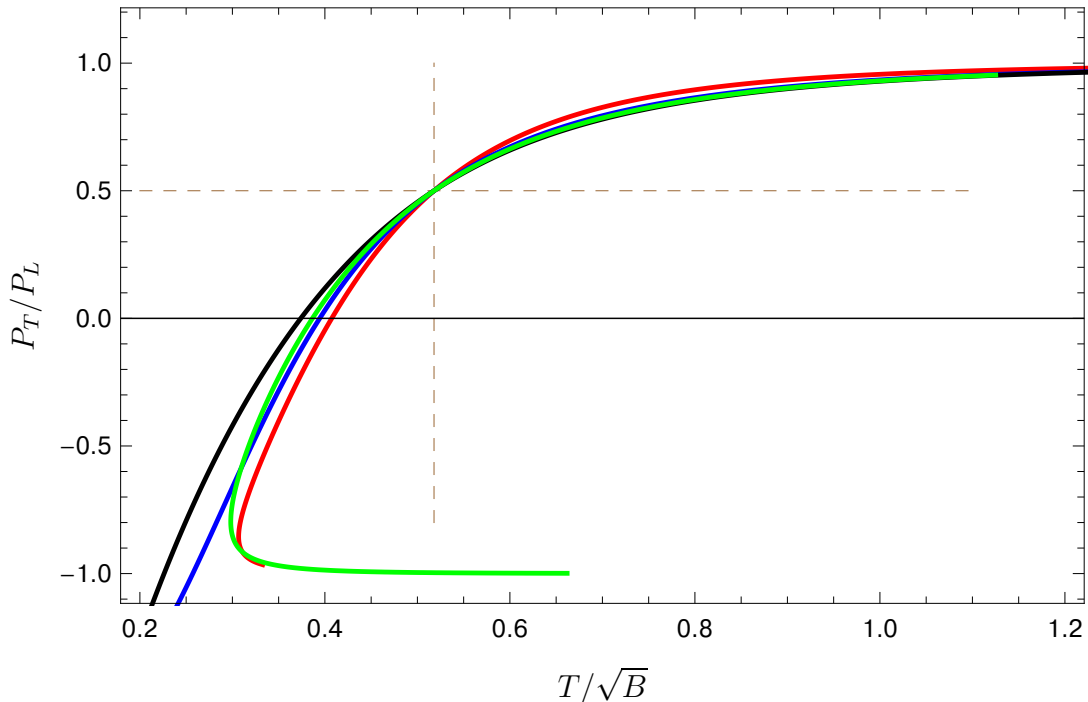


Figure 2: Renormalization scale δ is adjusted separately for the \mathbb{CFT}_{diag} , \mathbb{CFT}_{STU} and $\mathbb{CFT}_{PW,m=0}$ models (see (1.7)) to ensure that in all these models the pressure anisotropy $R = 0.5$ occurs for the same value of $\frac{T}{\sqrt{B}}$ as in the $\mathbb{CFT}_{PW,m=\infty}$ model (see (1.6)). This matching point is highlighted with the dashed brown lines.

curves exhibit the same high-temperature asymptotics, the anisotropy parameter R is quite sensitive to δ ; in fact, $R_{\mathbb{CFT}_{diag}}$ diverges for $\delta = 2.5$ (because P_L crosses zero with P_T remaining finite). Varying δ , it is easy to achieve $R_{\mathbb{CFT}_{diag}}$, $R_{\mathbb{CFT}_{STU}}$ and $R_{\mathbb{CFT}_{PW,m=0}}$ in the IR to be “to the left” of the scheme-independent (red) curve $R_{\mathbb{CFT}_{PW,m=\infty}}$ (top panels and the bottom left panel); or ”to the right” of the scheme-independent (red) curve $R_{\mathbb{CFT}_{PW,m=\infty}}$ (the bottom right panel).

In Fig. 1 we kept δ the same for the conformal models \mathbb{CFT}_{diag} , \mathbb{CFT}_{STU} and $\mathbb{CFT}_{PW,m=0}$. This is very reasonable given that one can match δ across all the models by comparing the UV, *i.e.*, $T/\sqrt{B} \gg 1$ thermodynamics (see appendix B) — there are no other scales besides T and B , and thus by dimensional analysis¹⁰,

$$P_{T/L} = T^4 \hat{P}_{T/L} \left(\frac{T}{\sqrt{B}}, \frac{\mu}{\sqrt{B}} \right). \quad (1.5)$$

¹⁰The asymptotic AdS_5 radius L always scales out from the final formulas.

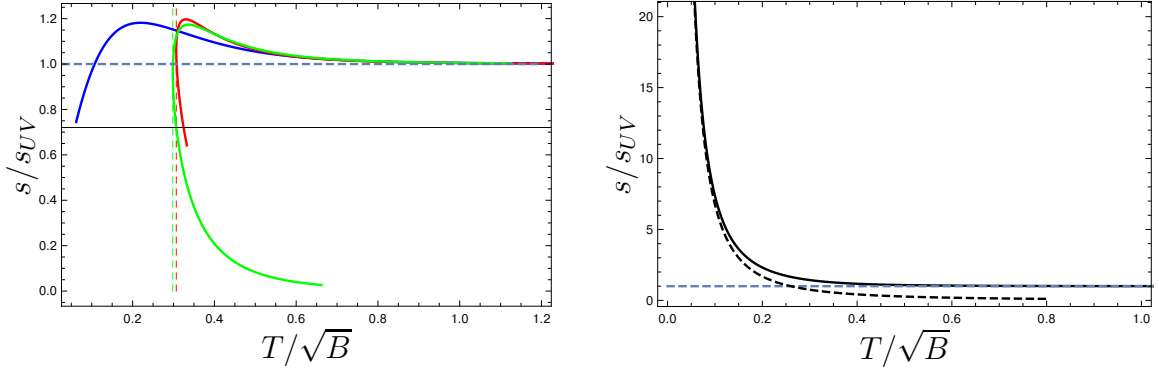


Figure 3: Entropy densities s in conformal models, relative to the entropy densities of the UV fixed points s_{UV} at the corresponding temperature (see (1.8)), as functions of T/\sqrt{B} : CFT_{diag} (black), CFT_{STU} (blue), $\text{CFT}_{PW,m=0}$ (green) and $\text{CFT}_{PW,m=\infty}$ (red). Left panel: vertical dashed lines indicate critical temperatures T_{crit} separating thermodynamically stable and unstable phases of $\text{CFT}_{PW,m=0}$ (green) and $\text{CFT}_{PW,m=\infty}$ (red) models. Right panel: the dashed black line is the small- T asymptote of the relative entropy in the CFT_{diag} model, see (1.9).

If we give up on maintaining the same renormalization scale for all the conformal models, it is easy to 'collapse' all the curves for the pressure anisotropy, see Fig. 2. We will not perform sophisticated fits as in [1], and instead, adjusting δ independently for each model, we require that in all models the pressure anisotropy $R = 0.5$ is attained at the same value of T/\sqrt{B} (represented by the dashed brown lines):

$$\left. \frac{T}{\sqrt{B}} \right|_{\text{CFT}_{diag}, \text{CFT}_{STU}, \text{CFT}_{PW,m=0}} = \left. \frac{T}{\sqrt{B}} \right|_{\text{CFT}_{PW,m=\infty}} = 0.51796(7). \quad (1.6)$$

Specifically, we find that (1.6) is true, provided

$$\{\delta_{\text{CFT}_{STU}}, \delta_{\text{CFT}_{diag}}, \delta_{\text{CFT}_{PW,m=0}}\} = \{3.9592(4), 4.2662(0), 4.1659(8)\}. \quad (1.7)$$

In a nutshell, this is what was done in [1] to claim a universal magnetoresponse for $R \gtrsim 0.5$. Rather, we interpret the collapse in Fig. 2 as nothing but a fitting artifact, possible due to a strong dependence of the anisotropy parameter R on the renormalization scale.

To further see that there is no universal physics, we can compare renormalization scheme-independent anisotropic thermodynamic quantities of the models: the entropy densities, see Fig. 3. The color coding is as before: CFT_{diag} (black curves), CFT_{STU} (blue curves), $\text{CFT}_{PW,m=0}$ (green curves) and $\text{CFT}_{PW,m=\infty}$ (red curves). We plot the

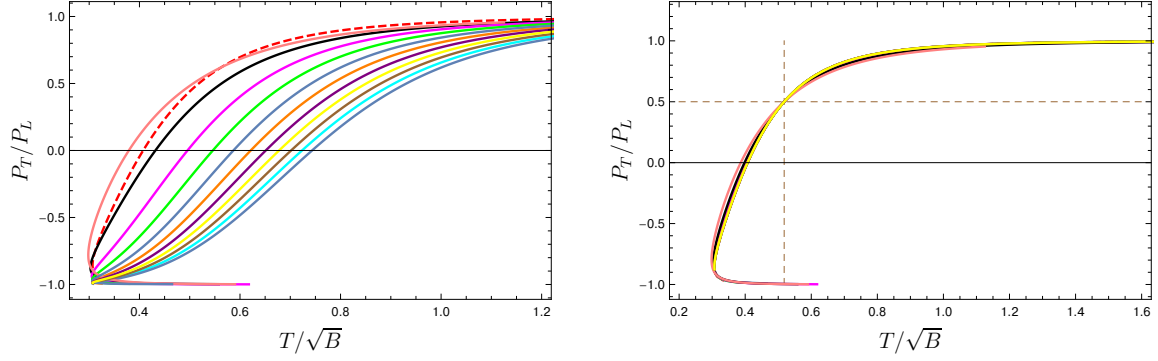


Figure 4: Anisotropy parameter $R = P_T/P_L$ for nonconformal models $n\text{CFT}_m$ for select values of the hypermultiplet mass m , see (1.10), as a function of T/\sqrt{B} (solid curves; from pink to dark blue as m increases). The dashed red curve is a benchmark model $\text{CFT}_{PW,m=\infty}$ — where the anisotropy parameter is renormalization scale independent. In the left panel the renormalization scale is set $\delta = 4$ for all $n\text{CFT}_m$ models; in the right panel it is separately adjusted for each $n\text{CFT}_m$ model to ensure that all the curves pass through the matching point, highlighted with dashed brown lines.

entropy densities relative to the entropy density of the UV fixed point at the corresponding temperature (see eq. (D.13) for the $\text{CFT}_{PW,m=\infty}$ model in [13]):

$$s_{UV} \Big|_{\text{CFT}_{diag}, \text{CFT}_{STU}, \text{CFT}_{PW,m=0}} = \frac{1}{2} \pi^2 N^2 T^3, \quad (m \times s_{UV}) \Big|_{\text{CFT}_{PW,m=\infty}} = \frac{432}{625} \pi^3 N^2 T^4. \quad (1.8)$$

The dashed vertical lines in the left panel indicate the terminal (critical temperature) T_{crit}/\sqrt{B} for $\text{CFT}_{PW,m=0}$ (green) and $\text{CFT}_{PW,m=\infty}$ (red) models which separates thermodynamically stable (top) and unstable (bottom) branches. Notice that s/s_{UV} diverges for the CFT_{diag} model as $T/\sqrt{B} \rightarrow 0$ — this is reflection of the IR BTZ-like thermodynamics (1.2); the dashed black line is the IR asymptote

$$\frac{s}{s_{UV}} \Big|_{\text{CFT}_{diag}} \rightarrow \frac{2}{3\pi^2} \frac{B}{T^2}, \quad \text{as} \quad \frac{T}{\sqrt{B}} \rightarrow 0. \quad (1.9)$$

In $n\text{CFT}_m$ models it is equally easy to 'collapse' the data for the pressure anisotropy. In these models we have an additional scale m — the mass of the $\mathcal{N} = 2$ hypermultiplet. In the absence of the magnetic field, *i.e.*, for isotropic $\mathcal{N} = 2^*$ plasma, the thermodynamics is renormalization scheme-independent¹¹ [20]. Once we turn on the

¹¹Scheme-dependence arises once we split the masses of the fermionic and bosonic components of

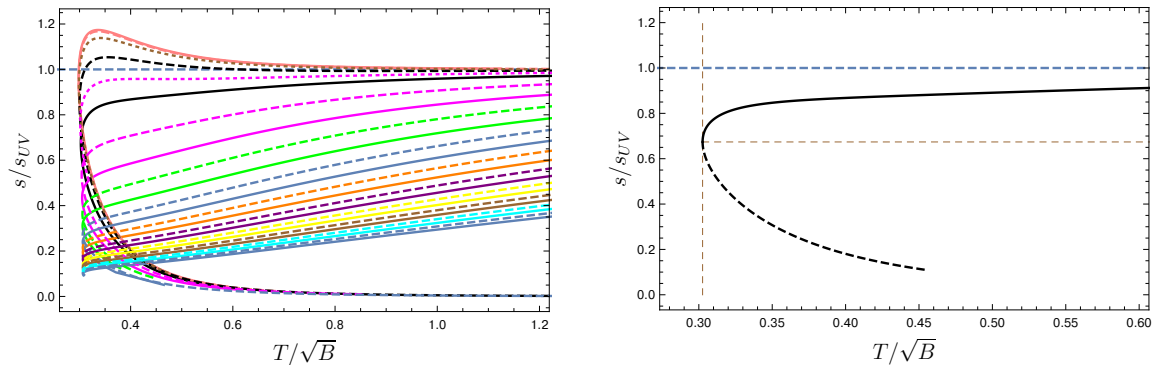


Figure 5: Left panel: entropy densities s in $n\mathbb{CFT}_m$ models, relative to the entropy density of the UV fixed point (the $\mathcal{N} = 4$ SYM in this case) s_{UV} at the corresponding temperature (see (1.8)), as functions of T/\sqrt{B} . Color coding of the solid curves agrees with that in Fig. 4 — see (1.10) for the set of the hypermultiplet masses. Additional dashed and dotted curves correspond to additional values of m , within the same interval (1.10). Each $n\mathbb{CFT}_m$ model has a terminal critical point. In the right panel we show this for the model with $m/\sqrt{2B} = 1$: the brown lines identify the critical temperature T_{crit}/\sqrt{B} and the relative entropy at the criticality s^{crit}/s_{UV} (these quantities are presented in Fig. 7). “Top” solid black curve denotes the thermodynamically stable branch and “bottom” dashed black curve denotes the thermodynamically unstable branch (see Fig. 6 for further details).

magnetic field, there is a scheme-dependence. In Fig. 4 we show the pressure anisotropy for $\mathcal{N} = 2^*$ gauge theory for select values of m (solid curves from pink to dark blue),

$$\frac{m}{\sqrt{2B}} = \left\{ \frac{1}{100}, 1, 2, 3, 4, 5, 6, 7, 8, 9, 10 \right\}. \quad (1.10)$$

The dashed red curve represents the anisotropy parameter of the conformal $\mathbb{CFT}_{PW, m=\infty}$ model, which is renormalization scheme-independent. In the left panel the renormalization scale $\delta = 4$ for all the $n\mathbb{CFT}_m$ models. In the right panel, we adjusted $\delta = \delta_m$ for each $n\mathbb{CFT}_m$ model independently, so that the pressure anisotropy $R_{n\mathbb{CFT}_m} = 0.5$ at the same temperature as in the $\mathbb{CFT}_{PW, m=\infty}$ model, see (1.6). This matching point is denoted by dashed brown lines.

As in conformal models, the entropy densities (which are renormalization scheme independent thermodynamic quantities) are rather distinct, see left panel of Fig. 5. The $\mathcal{N} = 2^*$ hypermultiplet [20].

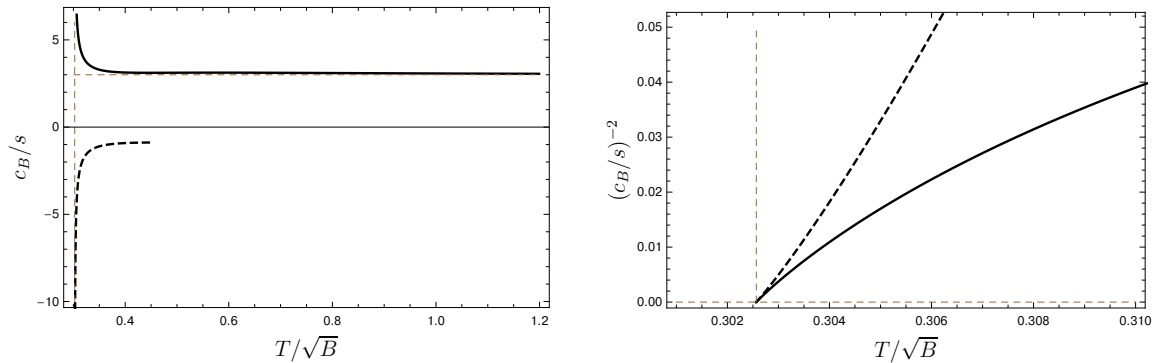


Figure 6: $n\text{CFT}_m$ model with $m/\sqrt{2B} = 1$ is used to highlight phases of the anisotropic plasma. Following (1.3) we evaluate the constant- B specific heat of the plasma. The dashed brown lines highlight the location of the critical point. Left panel: the specific heat diverges as one approaches the critical temperature; it is negative for the branch denoted by the dashed black curve (see also the right panel of Fig. 5), indicating the thermodynamic instability. Right panel: $(c_B/s)^{-2}$ vanishes at criticality, with nonvanishing slope. This implies that the critical exponent $\alpha = \frac{1}{2}$, see (1.11).

color coding is as in Fig. 4, except that we collected more data¹² in addition to (1.10): these are the dashed and dotted curves. The entropy density of the UV fixed point is defined as in (1.8). All the $n\text{CFT}_m$ models studied, as well as the $\text{CFT}_{PW,m=0}$ and $\text{CFT}_{PW,m=\infty}$ conformal models, have a terminal critical point T_{crit} that separates the thermodynamically stable (top solid) and unstable (bottom dashed) branches, which we presented for the $\frac{m}{\sqrt{2B}} = 1$ $n\text{CFT}_m$ model in the right panel. The dashed brown lines identify the critical temperature T_{crit} and the entropy density s^{crit} at criticality. In Fig. 6 we present results for the specific heat c_B in this model defined as in (1.3). Indeed, the (lower) thermodynamically unstable branch has a negative specific heat (left panel); approaching the critical temperature from above we observe the divergence in the specific heat, both for the stable and the unstable branches. To extract a critical exponent α , defined as

$$c_B \propto \left(\frac{T}{T_{crit}} - 1 \right)^{-\alpha}, \quad T \rightarrow T_{crit} + 0, \quad (1.11)$$

we plot (right panel) the dimensionless quantity c_B^2/s^2 as a function of T/\sqrt{B} . Both the stable (solid) and the unstable (dashed) curves approach zero, signaling the divergence

¹²To have a better characterization of the critical points.

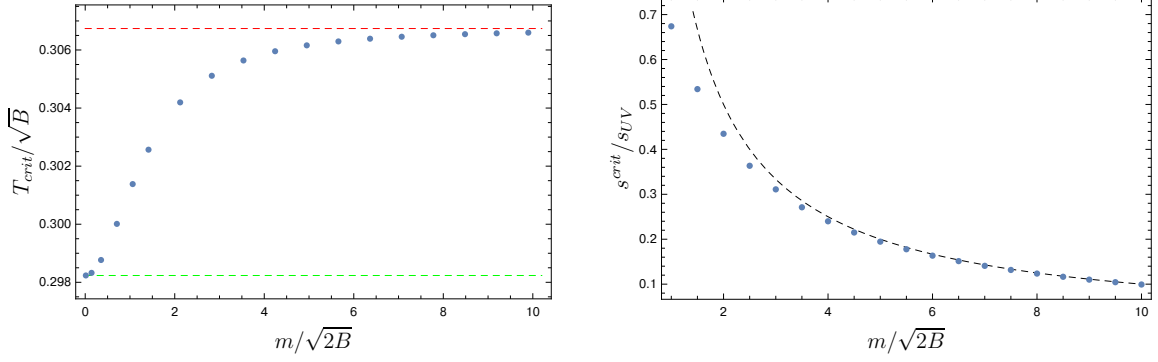


Figure 7: $n\text{CFT}_m$ models as well as the conformal models $\text{CFT}_{PW,m=0}$ and $\text{CFT}_{PW,m=\infty}$ have terminal critical temperature, separating thermodynamically stable and unstable phases. In the left panel we present T_{crit}/\sqrt{B} as function of $m/\sqrt{2B}$; in the right panel we present the relative entropy at criticality $\gamma = s^{crit}/s_{UV}$ (1.13). The dots represent results for the $n\text{CFT}_m$ models; the dashed horizontal lines (left panel) represent the critical temperature for the $\text{CFT}_{PW,m=0}$ model (green) and the $\text{CFT}_{PW,m=\infty}$ model (red). The dashed black curve (right panel) represents the asymptote of γ as $m/\sqrt{B} \rightarrow \infty$, see (1.14).

of the specific heat at the critical temperature (vertical dashed brown line), with a finite slope — this implies that the critical exponent is

$$\alpha = \frac{1}{2}. \quad (1.12)$$

There is a remarkable universality of the critical points in $n\text{CFT}_m$ and conformal $\text{CFT}_{PW,m=0}$ and $\text{CFT}_{PW,m=\infty}$ models. In Fig. 7 (left panel) we present the results for the critical temperature as a function of $m/\sqrt{2B}$ in $n\text{CFT}_m$ models (points). The horizontal dashed lines indicate the location of the critical points for the $\text{CFT}_{PW,m=0}$ (green) and $\text{CFT}_{PW,m=\infty}$ (red) conformal models. In the right panel the dots represent the relative entropy,

$$\gamma = \gamma(m/\sqrt{B}) \equiv \frac{s^{crit}}{s_{UV}}, \quad (1.13)$$

at criticality for the $n\text{CFT}_m$ models. Effectively, γ as in (1.13) measures the number of DOF at critical point in anisotropic plasma relative to the number of DOF (or the central charge) of the UV fixed point ($\mathcal{N} = 4$ SYM). The dashed black line is a simple asymptotic for γ as $m/\sqrt{B} \rightarrow \infty$, γ_∞ ,

$$\gamma_\infty = \frac{\sqrt{2B}}{m}. \quad (1.14)$$

One can understand the origin of the asymptote (1.13) from the fact that $n\text{CFT}_m$ models in the large m limit should resemble the conformal model $\text{CFT}_{PW,m=\infty}$; thus, we expect that $\gamma_\infty \approx \gamma_{\text{CFT}_{PW,m=\infty}}$. Indeed,

$$\begin{aligned}
\gamma_{\text{CFT}_{PW,m=\infty}} &= \frac{s_{\text{CFT}_{PW,m=\infty}}^{crit}}{s_{UV,\text{CFT}_{diag}}} = \underbrace{\frac{s^{crit}}{s_{UV}}}_{1.0603(7)} \times \underbrace{\frac{s_{UV,\text{CFT}_{PW,m=\infty}}}{s_{UV,\text{CFT}_{diag}}}}_{\frac{864\pi}{625} \times \frac{T_{crit}}{m}} \\
&= 1.0603(7) \times \frac{864\pi}{625\sqrt{2}} \times \underbrace{\frac{T_{crit}}{\sqrt{B}}}_{0.30673(9)} \times \frac{\sqrt{2B}}{m} = 0.99883(9) \times \frac{\sqrt{2B}}{m},
\end{aligned} \tag{1.15}$$

where we extracted numerically the value of $\frac{s^{crit}}{s_{UV}}$ for the $\text{CFT}_{PW,m=\infty}$ conformal model, used (1.8) to analytically compute the second factor in the first line, and substituted the numerical value for T_{crit}/\sqrt{B} of the $\text{CFT}_{PW,m=\infty}$ model in the second line.

We now outline the rest of the paper, containing technical details necessary to obtain the results reported above. In section 2 we introduce the holographic theory of [7] and explain how the various models discussed here arise as consistent truncations of the latter: CFT_{diag} in section 2.1, CFT_{STU} in section 2.2, and $n\text{CFT}_m$ in section 2.3. The conformal models $\text{CFT}_{PW,m=0}$ and $\text{CFT}_{PW,m=\infty}$ are special limits of the $n\text{CFT}_m$ model and are discussed in sections 2.3.1 and 2.3.2 correspondingly. Holographic renormalization is by now a standard technique [21], and we only present the results for the boundary gauge theory observables. Our work is heavily numerical. It is thus important to validate the numerical results in the limits where perturbative computations (analytical or numerical) are available. We have performed such validations in appendix B, *i.e.*, when $\frac{T}{\sqrt{B}} \gg 1$. We did not want to overburden the reader with details, and so we did not present the checks of the agreement of the numerical parameters (*e.g.*, as in (2.23)) with the corresponding perturbative counterparts — but we have performed such checks in all models. There are further important constraints on the numerically obtained energy density, pressure, entropy, etc., of the anisotropic plasma: the first law of the thermodynamics $d\mathcal{E} = Tds$ (at constant magnetic field and the mass parameter, if available), and the thermodynamic relation between the free energy density and the longitudinal pressure $\mathcal{F} = -P_L$. The latter relation can be proved (see appendix A) at the level of the equations of motion, borrowing the holographic arguments of [22] used to establish the universality of the shear viscosity to the entropy

density in the holographic plasma models. Still, as the first law of thermodynamics, it provides an important consistency check on the numerical data — we verified these constraints in all the models, both perturbatively in the high-temperature limit, to $\mathcal{O}\left(\frac{B^4}{T^8}\right)$ inclusive, see appendix B, and for finite values of B/\sqrt{T} , see appendix C — once again, we present only partial results of the full checks.

Our paper is a step in broadening the class of strongly coupled magnetized gauge theory plasmas (both conformal and massive) amenable to controlled holographic analysis. We focused on the equation of state, extending the work of [1]. The next step is to analyze the magneto-transport in these models, in particular the magneto-transport at criticality.

2 Technical details

The starting point for the holographic analysis is the effective action of [7]:

$$\begin{aligned}
S_5 = & \frac{1}{4\pi G_5} \int_{\mathcal{M}_5} d^5\xi \sqrt{-g} \left[\frac{R}{4} - \frac{1}{4} \left(\rho^4 \nu^{-4} F_{\mu\nu}^{(1)} F^{(1)\mu\nu} + \rho^4 \nu^4 F_{\mu\nu}^{(2)} F^{(2)\mu\nu} + \rho^{-8} F_{\mu\nu}^{(3)} F^{(3)\mu\nu} \right) \right. \\
& - \frac{1}{2} \sum_{j=1}^4 (\partial_\mu \phi_j)^2 - 3 (\partial_\mu \alpha)^2 - (\partial_\mu \beta)^2 - \frac{1}{8} \sinh^2(2\phi_1) (\partial_\mu \theta_1 + (A_\mu^{(1)} + A_\mu^{(2)} - A_\mu^{(3)}))^2 \\
& - \frac{1}{8} \sinh^2(2\phi_2) (\partial_\mu \theta_2 + (A_\mu^{(1)} - A_\mu^{(2)} + A_\mu^{(3)}))^2 - \frac{1}{8} \sinh^2(2\phi_3) (\partial_\mu \theta_3 + (-A_\mu^{(1)} + A_\mu^{(2)} \\
& \left. + A_\mu^{(3)}))^2 - \frac{1}{8} \sinh^2(2\phi_4) (\partial_\mu \theta_4 - (A_\mu^{(1)} + A_\mu^{(2)} + A_\mu^{(3)}))^2 - \mathcal{P} \right], \tag{2.1}
\end{aligned}$$

where the $F^{(J)}$ are the field strengths of the $U(1)$ gauge fields, $A^{(J)}$, and \mathcal{P} is the scalar potential. We introduced

$$\rho \equiv e^\alpha, \quad \nu \equiv e^\beta. \tag{2.2}$$

The scalar potential, \mathcal{P} , is given in terms of a superpotential

$$\mathcal{P} = \frac{g^2}{8} \left[\sum_{j=1}^4 \left(\frac{\partial W}{\partial \phi_j} \right)^2 + \frac{1}{6} \left(\frac{\partial W}{\partial \alpha} \right)^2 + \frac{1}{2} \left(\frac{\partial W}{\partial \beta} \right)^2 \right] - \frac{g^2}{3} W^2, \tag{2.3}$$

where

$$\begin{aligned}
W = & - \frac{1}{4\rho^2\nu^2} \left[(1 + \nu^4 - \nu^2\rho^6) \cosh(2\phi_1) + (-1 + \nu^4 + \nu^2\rho^6) \cosh(2\phi_2) \right. \\
& \left. + (1 - \nu^4 + \nu^2\rho^6) \cosh(2\phi_3) + (1 + \nu^4 + \nu^2\rho^6) \cosh(2\phi_4) \right]. \tag{2.4}
\end{aligned}$$

In what follows we set gauged supergravity coupling $g = 1$, this corresponds to setting the asymptotic AdS_5 radius to $L = 2$. The five dimensional gravitational constant G_5 is related to the rank of the supersymmetric $\mathcal{N} = 4$ $SU(N)$ UV fixed point as

$$G_5 = \frac{4\pi}{N^2}. \quad (2.5)$$

The models discussed below, *i.e.*, \mathbb{CFT}_{diag} , \mathbb{CFT}_{STU} and $n\mathbb{CFT}_m$, have holographic duals which are consistent truncations of (2.1). It would be interesting to study the stability of these truncations following [23].

2.1 \mathbb{CFT}_{diag}

The holographic dual to the \mathbb{CFT}_{diag} conformal model is a consistent truncation of (2.1) with

$$\alpha = \beta = \phi_j = \theta_j = 0, \quad A_\mu^{(1)} = A_\mu^{(2)} = A_\mu^{(3)} = \frac{2}{\sqrt{3}} A_\mu, \quad (2.6)$$

leading to

$$S_{\mathbb{CFT}_{diag}} = \frac{1}{16\pi G_5} \int_{\mathcal{M}_5} d^5\xi \sqrt{-g} \left[R - 4F_{\mu\nu}F^{\mu\nu} + 3 \right], \quad (2.7)$$

where we used the normalization of the bulk $U(1)$ to be consistent with [1].

This model has been extensively studied in [1, 4] and we do not review it here.

2.2 \mathbb{CFT}_{STU}

The holographic dual to the \mathbb{CFT}_{STU} is a special case of the STU model [10, 11, 24], a consistent truncation of the effective action (2.1) with

$$\theta_j = \phi_j = 0, \quad (2.8)$$

leading to

$$S_{STU} = \frac{1}{4\pi G_5} \int_{\mathcal{M}_5} d^5\xi \sqrt{-g} \left[\frac{R}{4} - \frac{1}{4} \left(\rho^4 \nu^{-4} F_{\mu\nu}^{(1)} F^{(1)\mu\nu} + \rho^4 \nu^4 F_{\mu\nu}^{(2)} F^{(2)\mu\nu} + \rho^{-8} F_{\mu\nu}^{(3)} F^{(3)\mu\nu} \right) - 3(\partial_\mu \alpha)^2 - (\partial_\mu \beta)^2 - \mathcal{P}_{STU} \right], \quad (2.9)$$

and the scalar potential

$$\mathcal{P}_{STU} = -\frac{1}{4}(\rho^2 \nu^2 + \rho^2 \nu^{-2} + \rho^{-4}). \quad (2.10)$$

We would like to keep a single bulk gauge field, so we can set two of them to zero and work with the remaining one. The symmetries of the action allow us to choose whichever gauge field we want. To see this, notice that the action (2.9) is invariant under $F_{\mu\nu}^{(1)} \rightarrow F_{\mu\nu}^{(2)}$ together with $\nu \rightarrow \nu^{-1}$. Moreover, (2.9) with $F_{\mu\nu}^{(1)} \equiv 2F_{\mu\nu}$ and $F_{\mu\nu}^{(2)} = F_{\mu\nu}^{(3)} = 0$ is the same as with $F_{\mu\nu}^{(3)} \equiv 2F_{\mu\nu}$ and $F_{\mu\nu}^{(1)} = F_{\mu\nu}^{(2)} = 0$ for the gauge fields and with the scalar field redefinitions $\rho \rightarrow \nu^{1/2}\rho^{-1/2}$ and $\nu \rightarrow \nu^{1/2}\rho^{1/2}$. Thus, we arrive to the holographic dual of \mathbb{CFT}_{STU} as

$$S_{\mathbb{CFT}_{STU}} = \frac{1}{4\pi G_5} \int_{\mathcal{M}_5} d^5\xi \sqrt{-g} \left[\frac{R}{4} - \rho^4 \nu^{-4} F_{\mu\nu} F^{\mu\nu} - 3(\partial_\mu \alpha)^2 - (\partial_\mu \beta)^2 - \mathcal{P}_{STU} \right], \quad (2.11)$$

where once again we used the normalization of the remaining gauge field as in [1].

Solutions to the gravitational theory (2.11) representing magnetic black branes dual to anisotropic magnetized \mathbb{CFT}_{STU} plasma correspond to the following background ansatz¹³:

$$ds_5^2 = -c_1^2 dt^2 + c_2^2 (dx^2 + dy^2) + \left(\frac{r}{2}\right)^2 dz^2 + c_4^2 dr^2, \quad F = B dx \wedge dy, \quad (2.12)$$

where all the metric warp factors c_i as well as the bulk scalars ρ and ν are functions of the radial coordinate r ,

$$r \in [r_0, +\infty), \quad (2.13)$$

where r_0 is a location of a regular Schwarzschild horizon, and $r \rightarrow +\infty$ is the asymptotic AdS_5 boundary. Introducing a new radial coordinate

$$x \equiv \frac{r_0}{r}, \quad x \in (0, 1], \quad (2.14)$$

and denoting

$$c_1 = \frac{r}{2} \left(1 - \frac{r_0^4}{r^4}\right)^{1/2} a_1, \quad c_2 = \frac{r}{2} a_2, \quad c_4 = \frac{2}{r} \left(1 - \frac{r_0^4}{r^4}\right)^{-1/2} a_4 \quad (2.15)$$

$$B = \frac{1}{2} r_0^2 b,$$

¹³Note that we fixed the radial coordinate r with the choice of the metric warp factor in front of dz^2 .

we obtain the following system of ODEs (in a radial coordinate x , $' = \frac{d}{dx}$):

$$0 = a_1' + \frac{a_1}{\nu^4 \rho^4 a_2^3 x (3a_2 - 2a_2' x) (1 - x^4)} \left(\nu^4 \rho^4 a_2^2 x a_2' ((x^4 - 1) x a_2' - 2(x^4 - 3) a_2) \right. \\ \left. - 2\nu^2 \rho^2 a_2^4 x^2 (x^4 - 1) (3\nu^2 (\rho')^2 + \rho^2 (\nu')^2) - 256 \rho^8 a_4^2 x^4 b^2 + 2\nu^2 a_2^4 (a_4^2 (\nu^4 \rho^6 + \rho^6 + \nu^2) \right. \\ \left. - 3\nu^2 \rho^4) \right), \quad (2.16)$$

$$0 = a_4' + \frac{a_4}{3\nu^4 \rho^4 a_2^4 x (3a_2 - 2a_2' x) (x^4 - 1)} \left(9\nu^4 \rho^4 a_2^3 x^2 (x^4 - 1) (a_2')^2 + 6\nu^2 \rho^2 a_2^5 x^2 (x^4 - 1) \right. \\ \times (3\nu^2 (\rho')^2 + \rho^2 (\nu')^2) + 256 a_4^2 \rho^8 x^4 (9a_2 - 4a_2' x) b^2 - 4\nu^2 a_2^4 x (2a_4^2 (\nu^4 \rho^6 + \rho^6 + \nu^2) \\ \left. + 3\nu^2 \rho^4 (x^4 - 2)) a_2' + 6\nu^2 a_2^5 (a_4^2 (\nu^4 \rho^6 + \rho^6 + \nu^2) - 3\nu^2 \rho^4) \right), \quad (2.17)$$

$$0 = a_2'' - \frac{(a_2')^2}{a_2} - \frac{512 a_4^2 \rho^4 x^2 (3a_2 - a_2' x) b^2}{3\nu^4 a_2^4 (x^4 - 1)} + \frac{a_2'}{3x \rho^4 \nu^2 (x^4 - 1)} \left(4a_4^2 (\rho^6 \nu^4 + \rho^6 + \nu^2) \right. \\ \left. + 3\rho^4 \nu^2 (x^4 - 1) \right), \quad (2.18)$$

$$0 = \rho'' - \frac{(\rho')^2}{\rho} + \frac{256 a_4^2 \rho^4 x^2 (2\rho' x + \rho) b^2}{3\nu^4 a_2^4 (x^4 - 1)} + \frac{\rho'}{3x \nu^2 \rho^4 (x^4 - 1)} \left(4a_4^2 (\rho^6 \nu^4 + \rho^6 + \nu^2) \right. \\ \left. + 3\rho^4 \nu^2 (x^4 - 1) \right) - \frac{a_4^2 (\rho^6 \nu^4 + \rho^6 - 2\nu^2)}{3\rho^3 \nu^2 x^2 (x^4 - 1)}, \quad (2.19)$$

$$0 = \nu'' - \frac{(\nu')^2}{\nu} - \frac{256 a_4^2 \rho^4 x^2 (3\nu - 2\nu' x) b^2}{3\nu^4 a_2^4 (x^4 - 1)} + \frac{\nu'}{3\rho^4 \nu^2 x (x^4 - 1)} \left(4a_4^2 (\rho^6 \nu^4 + \rho^6 + \nu^2) \right. \\ \left. + 3\rho^4 \nu^2 (x^4 - 1) \right) - \frac{a_4^2 \rho^2 (\nu^4 - 1)}{\nu x^2 (x^4 - 1)}. \quad (2.20)$$

Notice that r_0 is completely scaled out from all the equations of motion. Eqs. (2.16)-(2.20) have to be solved subject to the following asymptotics:

- in the UV, *i.e.*, as $x \rightarrow 0_+$,

$$a_1 = 1 + a_{1,2} x^4 + \mathcal{O}(x^8 \ln x), \quad a_2 = 1 + (a_{2,2} - 32b^2 \ln x) x^4 + \mathcal{O}(x^6), \\ a_4 = 1 + \left(-a_{1,2} + \frac{64}{3} b^2 - \frac{4}{3} n_1^2 - 4r_1^2 - 2a_{2,2} + 64b^2 \ln x \right) x^4 + \mathcal{O}(x^6), \quad (2.21) \\ \rho = 1 + r_1 x^2 + \mathcal{O}(x^4), \quad \nu = 1 + n_1 x^2 + \mathcal{O}(x^4);$$

■ in the IR, *i.e.*, as $y \equiv 1 - x \rightarrow 0_+$,

$$\begin{aligned}
a_1 &= a_{1,h,0} + \mathcal{O}(y), & a_2 &= a_{2,h,0} + \mathcal{O}(y), & \rho &= r_{h,0} + \mathcal{O}(y), & \nu &= n_{h,0} + \mathcal{O}(y), \\
a_4 &= \frac{3a_{2,h,0}^2 r_{h,0}^2 n_{h,0}^2}{(3a_{2,h,0}^4 n_{h,0}^6 r_{h,0}^6 + 3a_{2,h,0}^4 n_{h,0}^2 r_{h,0}^6 + 96b^2 r_{h,0}^8 + 3a_{2,h,0}^4 n_{h,0}^4)^{1/2}} + \mathcal{O}(y).
\end{aligned}
\tag{2.22}$$

In total, given b — roughly the ratio $\frac{\sqrt{B}}{T}$, the asymptotic expansions are specified by 8 parameters:

$$\{a_{1,2}, a_{2,2}, r_1, n_1, a_{1,h,0}, a_{2,h,0}, r_{h,0}, n_{h,0}\}, \tag{2.23}$$

which is the correct number of parameters necessary to provide a solution to a system of three second order and two first order equations, $3 \times 2 + 2 \times 1 = 8$. The parameters n_1 and r_1 correspond to the expectation value of two dimension $\Delta = 2$ operators of the boundary \mathbb{CFT}_{STU} ; the other two parameters, $a_{1,2}$ and $a_{2,2}$, determine the expectation value of its stress-energy tensor. Using the standard holographic renormalization we find:

$$\begin{aligned}
\langle T_{tt} \rangle &\equiv \mathcal{E} = \frac{r_0^4}{512\pi G_5} (3 - 6a_{1,2} - 128b^2 \ln r_0 + 128b^2 \ln 2 + 4a_{2,2} + 64b^2 \kappa), \\
\langle T_{xx} \rangle &= \langle T_{yy} \rangle \equiv P_T = \frac{r_0^4}{512\pi G_5} (3 - 6a_{1,2} - 128b^2 \ln r_0 + 128b^2 \ln 2 + 4a_{2,2} + 64b^2 \kappa), \\
\langle T_{zz} \rangle &\equiv P_L = \frac{r_0^4}{512\pi G_5} (3 - 6a_{1,2} - 128b^2 \ln r_0 + 128b^2 \ln 2 + 4a_{2,2} + 64b^2 \kappa),
\end{aligned}
\tag{2.24}$$

for the components of the boundary stress-energy tensor, and

$$s = \frac{r_0^3 a_{2,h,0}^2}{32G_5}, \quad T = \frac{\sqrt{3} [a_{2,h,0}^4 n_{h,0}^2 (n_{h,0}^4 r_{h,0}^6 + r_{h,0}^6 + n_{h,0}^2) + 32b^2 r_{h,0}^8]^{1/2} a_{1,h,0} r_0}{12\pi r_{h,0}^2 n_{h,0}^2 a_{2,h,0}^2}, \tag{2.25}$$

for the entropy density and the temperature. Note that, as in $\mathcal{N} = 4$ SYM [1],

$$\langle T^\mu{}_\mu \rangle = -\frac{r_0^4 b^2}{4\pi G_5} = -\frac{N^2}{4\pi^2} B^2, \tag{2.26}$$

where we used (2.15) and (2.5). The (holographic) free energy density is given by the standard relation

$$\mathcal{F} = \mathcal{E} - Ts. \tag{2.27}$$

The constant parameter κ in (2.24) comes from the finite counterterm of the holographic renormalization; we find it convenient to relate it to the renormalization scale μ in (1.4) as

$$\kappa = 2 \ln(2\pi\mu). \quad (2.28)$$

As shown in appendix B.1, the renormalization scheme choice (2.28) implies that in the high-temperature limit $T^2 \gg B$,

$$R_{\text{CFT}_{STU}} = 1 - \frac{4B^2}{\pi^4 T^4} \ln \frac{T}{\mu\sqrt{2}} + \mathcal{O}\left(\frac{B^4}{T^8} \ln^2 \frac{T}{\mu}\right). \quad (2.29)$$

We can not solve the equations (2.16)-(2.20) analytically; adapting numerical techniques developed in [25], we solve these equations (subject to the asymptotics (2.21) and (2.22)) numerically. The results of numerical analysis are data files assembled of parameters (2.23), labeled by b . It is important to validate the numerical data (in addition to the standard error analysis). There are two important constraints that we verified for CFT_{STU} (and in fact all the other models):

- The first law of thermodynamics (FL), $d\mathcal{E}/(Tds) - 1$ (with B kept fixed), leads to the differential constrain on data sets (2.23) (here $' = \frac{d}{db}$):

$$\text{FL} : 0 = \frac{\sqrt{3}r_{h,0}^2 n_{h,0}^2 a_{2,h,0} ((2a'_{2,2} - 3a'_{1,2})b + 32b^2 + 6a_{1,2} - 4a_{2,2} - 3)}{(4a'_{2,h,0}b - 3a_{2,h,0})a_{1,h,0} \sqrt{a_{2,h,0}^4 n_{h,0}^2 ((n_{h,0}^4 + 1)r_{h,0}^6 + n_{h,0}^2) + 32b^2 r_{h,0}^8}} - 1. \quad (2.30)$$

- Anisotropy introduced by the external magnetic field results in $P_T \neq P_L$. From the elementary anisotropic thermodynamics (see [1] for a recent review), the free energy density of the system \mathcal{F} is given by

$$\mathcal{F} = -P_L \quad \implies \quad 0 = \frac{\mathcal{E} + P_L}{sT} - 1. \quad (2.31)$$

We emphasize that holographic renormalization (even anisotropic one) naturally enforces (2.27) (see [26] for one of the first demonstrations), but not (2.31). In appendix A we present a holographic proof¹⁴ of the thermodynamic relation (TR) (2.31). Applying it to CFT_{STU} model we arrive at the constraint

$$\text{TR} : 0 = \frac{\sqrt{3}(1 - 2a_{1,2})r_{h,0}^2 n_{h,0}^2}{a_{1,h,0} \sqrt{a_{2,h,0}^4 n_{h,0}^2 ((n_{h,0}^4 + 1)r_{h,0}^6 + n_{h,0}^2) + 32b^2 r_{h,0}^8}} - 1. \quad (2.32)$$

¹⁴The proof follows the same steps as in the first proof of the universality of the shear viscosity to the entropy density in holography [22].

In appendix B.1 we have verified FT and TR in the CFT_{STU} model to order $\mathcal{O}(b^4) \sim \mathcal{O}(B^4/T^8)$ inclusive¹⁵.

Technical details presented here are enough to generate the CFT_{STU} model plots reported in section 1.

2.3 $n\text{CFT}_m$

There is a simple consistent truncation of the effective action (2.1) to that of the PW action [8], supplemented with a single bulk $U(1)$ gauge field. Indeed, setting

$$\begin{aligned} \beta = 0 &\implies \nu = 1, & \phi_2 = \phi_3 &\equiv \chi, & \phi_1 = \phi_4 &= 0, \\ A^{(1)} = A^{(2)} &\equiv \sqrt{2}A, & A^{(3)} &= 0, & \theta_J &= 0. \end{aligned} \quad (2.33)$$

we find

$$S_{n\text{CFT}_m} = \frac{1}{4\pi G_5} \int_{\mathcal{M}_5} d^5\xi \sqrt{-g} \left[\frac{R}{4} - 3(\partial_\mu\alpha)^2 - (\partial_\mu\chi)^2 - \mathcal{P}_{PW} - \rho^4 F_{\mu\nu} F^{\mu\nu} \right], \quad (2.34)$$

where \mathcal{P}_{PW} is the Pilch-Warner scalar potential of the gauged supergravity:

$$\begin{aligned} \mathcal{P}_{PW} &= \frac{1}{48} \left(\frac{\partial W_{PW}}{\partial \alpha} \right)^2 + \frac{1}{16} \left(\frac{\partial W_{PW}}{\partial \chi} \right)^2 - \frac{1}{3} W_{PW}^2, \\ W_{PW} &= -\frac{1}{\rho^2} - \frac{1}{2} \rho^4 \cosh(2\chi). \end{aligned} \quad (2.35)$$

We use the same holographic background ansatz, the same radial coordinate x , as for the CFT_{STU} model (2.12)-(2.15); except that now we have the bulk scalar fields α and χ (here $' = \frac{d}{dx}$):

$$\begin{aligned} 0 &= a'_1 + \frac{2a_1 a_2 x}{3a_2 - 2a'_2 x} ((\chi')^2 + 3(\alpha')^2) + \frac{a_1 a'_2}{2a_2} - \frac{a_1(x^4 - 9)}{4x(x^4 - 1)} + \frac{64a_1 a_4^2 e^{4\alpha} x^3 b^2}{a_2^3 (3a_2 - 2a'_2 x)(x^4 - 1)} \\ &\quad - \frac{a_1 a_2 a_4^2}{8x(3a_2 - 2a'_2 x)(x^4 - 1)} \left(2e^{8\alpha} + 16e^{-4\alpha} - e^{8\alpha - 4\chi} + 16e^{2\alpha + 2\chi} + 16e^{2\alpha - 2\chi} - e^{8\alpha + 4\chi} \right) \\ &\quad + \frac{3a_1 a_2}{4x(3a_2 - 2a'_2 x)}, \end{aligned} \quad (2.36)$$

¹⁵Additionally, as in the $n\text{CFT}_m$ model with $m/\sqrt{2B} = 1$ (see appendix C), we checked both relations for finite b .

$$\begin{aligned}
0 = & a'_4 + \frac{2a_4a_2x}{3a_2 - 2a'_2x} ((\chi')^2 + 3(\alpha')^2) - \frac{3a_4a'_2}{2a_2} + \frac{64a_4^3e^{4\alpha}x^3(9a_2 - 4a'_2x)b^2}{3a_2^4(3a_2 - 2a'_2x)(x^4 - 1)} \\
& + \frac{a_4^3(3a_2 - 4xa'_2)}{24x(3a_2 - 2a'_2x)(x^4 - 1)} \left(2e^{8\alpha} + 16e^{2\alpha+2\chi} - e^{8\alpha-4\chi} + 16e^{2\alpha-2\chi} + 16e^{-4\alpha} - e^{8\alpha+4\chi} \right) \\
& - \frac{a_4(12a_2 - a'_2x(x^4 + 7)x)}{2(x^4 - 1)(3a_2 - 2a'_2x)x},
\end{aligned} \tag{2.37}$$

$$\begin{aligned}
0 = & a''_2 - \frac{(a'_2)^2}{a_2} - \frac{128a_4^2e^{4\alpha}x^2(3a_2 - a'_2x)b^2}{3a_2^4(x^4 - 1)} + \frac{a'_2}{12x(x^4 - 1)} \left(12(x^4 - 1) + a_4^2(2e^{8\alpha} \right. \\
& \left. + 16e^{2\alpha+2\chi} - e^{8\alpha-4\chi} + 16e^{2\alpha-2\chi} + 16e^{-4\alpha} - e^{8\alpha+4\chi}) \right),
\end{aligned} \tag{2.38}$$

$$\begin{aligned}
0 = & \alpha'' + \frac{64a_4^2e^{4\alpha}x^2(2\alpha'x + 1)b^2}{3a_2^4(x^4 - 1)} + \frac{\alpha'}{12x(x^4 - 1)} \left(12(x^4 - 1) + a_4^2(2e^{8\alpha} + 16e^{2\alpha+2\chi} \right. \\
& \left. - e^{8\alpha-4\chi} + 16e^{2\alpha-2\chi} + 16e^{-4\alpha} - e^{8\alpha+4\chi}) \right) - \frac{a_4^2}{12x^2(x^4 - 1)} \left(2e^{8\alpha} + 4e^{2\alpha+2\chi} - e^{8\alpha-4\chi} \right. \\
& \left. + 4e^{2\alpha-2\chi} - 8e^{-4\alpha} - e^{8\alpha+4\chi} \right),
\end{aligned} \tag{2.39}$$

$$\begin{aligned}
0 = & \chi'' + \frac{128a_4^2\chi'e^{4\alpha}x^3b^2}{3a_2^4(x^4 - 1)} + \frac{\chi'}{12x(x^4 - 1)} \left(12(x^4 - 1) + a_4^2(2e^{8\alpha} + 16e^{2\alpha+2\chi} - e^{8\alpha-4\chi} \right. \\
& \left. + 16e^{2\alpha-2\chi} + 16e^{-4\alpha} - e^{8\alpha+4\chi}) \right) - \frac{a_4^2(8e^{2\alpha+2\chi} + e^{8\alpha-4\chi} - 8e^{2\alpha-2\chi} - e^{8\alpha+4\chi})}{8x^2(x^4 - 1)}.
\end{aligned} \tag{2.40}$$

As in the \mathbb{CFT}_{STU} model, r_0 is completely scaled out from all the equations of motion. Eqs. (2.36)-(2.40) have to be solved subject to the following asymptotics:

- in the UV, *i.e.*, as $x \rightarrow 0_+$,

$$\begin{aligned}
a_1 &= 1 - x^4 \left(4\alpha_{1,0}^2 + 2\alpha_{1,0}\alpha_{1,1} + \frac{\alpha_{1,1}^2}{2} - \frac{64b^2}{3} + 2\chi_0\chi_{1,0} + 2a_{2,2,0} + a_{4,2,0} \right) + \mathcal{O}(x^6), \\
a_2 &= 1 + x^4 (-32b^2 \ln x + a_{2,2,0}) + \mathcal{O}(x^6 \ln x), \\
a_4 &= 1 - \frac{2}{3}x^2\chi_0^2 + x^4 \left(-4\alpha_{1,1}^2 \ln^2 x + \left(-8\alpha_{1,0}\alpha_{1,1} + 64b^2 - \frac{8}{3}\chi_0^4 - 2\alpha_{1,1}^2 \right) \ln x \right. \\
&\quad \left. + a_{4,2,0} \right) + \mathcal{O}(x^6 \ln^3 x), \\
\alpha &= x^2 (\alpha_{1,1} \ln x + \alpha_{1,0}) + \mathcal{O}(x^4 \ln^2 x), \\
\chi &= \chi_0 x + \left(\frac{4}{3}\chi_0^3 \ln x + \chi_{1,0} \right) x^3 + \mathcal{O}(x^5 \ln^2 x);
\end{aligned} \tag{2.41}$$

- in the IR, *i.e.*, as $y \equiv 1 - x \rightarrow 0_+$,

$$\begin{aligned}
a_1 &= a_{1,h,0} + \mathcal{O}(y), \quad a_2 = a_{2,h,0} + \mathcal{O}(y), \quad \alpha = \ln r_{h,0} + \mathcal{O}(y), \quad \chi = \ln c_{h,0} + \mathcal{O}(y), \\
a_4 &= 4\sqrt{3}a_{2,h,0}^2 r_{h,0}^2 c_{h,0}^2 \left(a_{2,h,0}^4 (r_{h,0}^6 (16c_{h,0}^6 - r_{h,0}^6 (1 - c_{h,0}^4)^2) + 16c_{h,0}^2 (r_{h,0}^6 + c_{h,0}^2)) \right. \\
&\quad \left. + 512b^2 c_{h,0}^4 r_{h,0}^8 \right)^{-1/2} + \mathcal{O}(y).
\end{aligned} \tag{2.42}$$

The non-normalizable coefficients $\alpha_{1,1}$ (of the dimension $\Delta = 2$ operator) and χ_0 (of the dimension $\Delta = 3$ operator) are related to the masses of the bosonic and the fermionic components of the hypermultiplet of $\mathcal{N} = 2^*$ gauge theory. When both masses are the same (see [20])

$$\alpha_{1,1} = \frac{2}{3} \chi_0^2. \tag{2.43}$$

Furthermore, carefully matching to the extremal PW solution [8,9] (following the same procedure as in [20]) we find

$$\frac{B}{m^2} = \frac{2b}{\chi_0^2}, \tag{2.44}$$

where m is the hypermultiplet mass. We find it convenient to use

$$\eta \equiv \frac{m}{\sqrt{2B}} \quad \implies \quad \chi_0 = 2\sqrt{b} \eta, \tag{2.45}$$

to label different mass parameters in $n\text{CFT}_m$ models, see (1.10). In total, given η and b , the asymptotics expansions are specified by 8 parameters:

$$\{a_{2,2,0}, a_{4,2,0}, \alpha_{1,0}, \chi_{1,0}, a_{1,h,0}, a_{2,h,0}, r_{h,0}, c_{h,0}\}, \tag{2.46}$$

which is the correct number of parameters necessary to provide a solution to a system of three second order and two first order equations, $3 \times 2 + 2 \times 1 = 8$. Parameters $\alpha_{1,0}$ and $\chi_{1,0}$ correspond to the expectation values of dimensions $\Delta = 2$ (\mathcal{O}_2) and $\Delta = 3$ (\mathcal{O}_3) operators (correspondingly) of the boundary $n\text{CFT}_m$; the other two parameters, $a_{2,2,0}$ and $a_{4,2,0}$, determine the expectation value of its stress-energy tensor. Using the standard holographic renormalization [27] we find:

$$\begin{aligned}
\langle T_{tt} \rangle \equiv \mathcal{E} &= \frac{r_0^4}{1536\pi G_5} \left(9 - 64b^2 (\eta^4 + 6 \ln r_0 - 6 \ln 2 - 3\kappa + 6) + 192\alpha_{1,0}b\eta^2 + 72\alpha_{1,0}^2 \right. \\
&\quad \left. + 48a_{2,2,0} + 18a_{4,2,0} + 48\sqrt{b}\eta\chi_{1,0} \right), \\
\langle T_{xx} \rangle = \langle T_{yy} \rangle \equiv P_T &= \frac{r_0^4}{4608\pi G_5} \left(9 - 64b^2(-7\eta^4 + 18 \ln r_0 - 18 \ln 2 - 9\kappa + 15) \right. \\
&\quad \left. - 192\alpha_{1,0}b\eta^2 + 72\alpha_{1,0}^2 + 144\sqrt{b}\eta\chi_{1,0} + 72a_{2,2,0} + 18a_{4,2,0} \right), \\
\langle T_{zz} \rangle \equiv P_L &= \frac{r_0^4}{4608\pi G_5} \left(9 + 64b^2 (7\eta^4 + 18 \ln r_0 - 18 \ln 2 - 9\kappa - 6) - 192\alpha_{1,0}b\eta^2 \right. \\
&\quad \left. + 72\alpha_{1,0}^2 + 144\sqrt{b}\eta\chi_{1,0} + 18a_{4,2,0} \right),
\end{aligned} \tag{2.47}$$

for the components of the boundary stress-energy tensor,

$$\mathcal{O}_2 = \frac{r_0^2}{8\pi G_5} \left(\alpha_{1,0} - \frac{2}{3}\eta^2 b \right), \quad \mathcal{O}_3 = -\frac{r_0^3}{16\pi G_5} \left(\chi_{1,0} + \frac{8}{3}\eta^3 b^{3/2} \right), \tag{2.48}$$

for the expectation values of the relevant operators, and

$$\begin{aligned}
s &= \frac{r_0^3 a_{2,h,0}^2}{32G_5}, \quad T = \frac{\sqrt{3}r_0 a_{1,h,0}}{48\pi a_{2,h,0}^2 c_{h,0}^2 r_{h,0}^2} \left[a_{2,h,0}^4 (16c_{h,0}^2 (r_{h,0}^6 + c_{h,0}^2) - r_{h,0}^6 ((c_{h,0}^4 - 1)^2 r_{h,0}^6 \right. \\
&\quad \left. - 16c_{h,0}^6)) + 512b^2 c_{h,0}^4 r_{h,0}^8 \right]^{1/2},
\end{aligned} \tag{2.49}$$

for the entropy density and the temperature. Note that, as expected [27],

$$\begin{aligned}
\langle T_{\mu}^{\mu} \rangle &= -\frac{r_0^4}{4\pi G_5} \left(b^2 \left(1 - \frac{4}{3}\eta^4 \right) + \alpha_{1,0}b\eta^2 - \frac{1}{4}\sqrt{b}\eta\chi_{1,0} \right) \\
&= -2m^2 \mathcal{O}_2 - m \mathcal{O}_3 - \frac{N^2}{4\pi^2} B^2,
\end{aligned} \tag{2.50}$$

where in the second equality we used (2.15), (2.5), (2.48) and (2.45). The (holographic) free energy density is directly given by the standard relation (2.27). The constant parameter κ in (2.47) comes from the finite counterterm of the holographic renormalization; we fix it as in (2.28).

We can not solve the equations (2.36)-(2.40) analytically; adapting numerical techniques developed in [25], we solve these equations (subject to the asymptotics (2.41) and (2.42)) numerically. The results of numerical analysis are data files assembled of parameters (2.46), labeled by b and η . As for the CFT_{STU} model, we validate the numerical data verifying the differential constraint from the first law of the thermodynamics $d\mathcal{E} = Tds$ (FL) and the algebraic constraint from the thermodynamic relation $\mathcal{F} = -P_L$ (TR):

$$\begin{aligned} \text{FL} : 0 = & \frac{4\sqrt{3}a_{2,h,0}c_{h,0}^2r_{h,0}^2}{a_{1,h,0}(3a_{2,h,0} - 4ba'_{2,h,0})} \left(8(4b\eta^2 + 3\alpha_{1,0})(\alpha_{1,0} - \alpha'_{1,0}b) - 4\sqrt{b}(2\chi'_{1,0}b - 3\chi_{1,0})\eta \right. \\ & \left. - 3a'_{4,2,0}b - 8a'_{2,2,0}b - 32b^2 + 6a_{4,2,0} + 16a_{2,2,0} + 3 \right) \left(a_{2,h,0}^4(16c_{h,0}^2(r_{h,0}^6 + c_{h,0}^2) \right. \\ & \left. - r_{h,0}^6((c_{h,0}^4 - 1)^2r_{h,0}^6 - 16c_{h,0}^6)) + 512b^2c_{h,0}^4r_{h,0}^8 \right)^{-1/2} - 1, \end{aligned} \quad (2.51)$$

$$\begin{aligned} \text{TR} : 0 = & \frac{4\sqrt{3}r_{h,0}^2c_{h,0}^2}{9a_{1,h,0}} \left(64b^2\eta^4 + 96\alpha_{1,0}b\eta^2 + 72\sqrt{b}\eta\chi_{1,0} + 72\alpha_{1,0}^2 - 384b^2 + 36a_{2,2,0} \right. \\ & \left. + 18a_{4,2,0} + 9 \right) \left(a_{2,h,0}^4(16c_{h,0}^2(r_{h,0}^6 + c_{h,0}^2) - r_{h,0}^6((c_{h,0}^4 - 1)^2r_{h,0}^6 - 16c_{h,0}^6)) \right. \\ & \left. + 512b^2c_{h,0}^4r_{h,0}^8 \right)^{-1/2} - 1. \end{aligned} \quad (2.52)$$

In appendix C we have verified FT and TR in the $n\text{CFT}_m$ model with $m/\sqrt{2B} = 1$ numerically.

Technical details presented here are enough to generate $n\text{CFT}_m$ model plots reported in section 1.

2.3.1 $\text{CFT}_{PW,m=0}$

The $\text{CFT}_{PW,m=0}$ model is a special case of the $n\text{CFT}_m$ model when the hypermultiplet mass m is set to zero. This necessitates setting the non-normalizable coefficients $\alpha_{1,1}$

and χ_0 to zero $\implies \eta = 0$ in (2.45). From (2.40) it is clear that this $m = 0$ limit is consistent with

$$\eta(x) \equiv 0 \quad \implies \quad \chi_{1,0} = 0, \quad (2.53)$$

implying that the \mathbb{Z}_2 symmetry of the holographic dual, *i.e.*, the symmetry associated with $\chi \leftrightarrow -\chi$, is unbroken. In what follows, we study the \mathbb{Z}_2 -symmetric phase of the $\text{CFT}_{PW,m=0}$ anisotropic thermodynamics¹⁶,

$$\mathcal{O}_3 = 0. \quad (2.54)$$

In appendix B.2 we verified FT and TR in $\text{CFT}_{PW,m=0}$ to order $\mathcal{O}(b^4)$ inclusive; we also present $\mathcal{O}(B^4/T^8)$ results for $R_{\text{CFT}_{PW,m=0}}$ and confirm that the renormalization scheme choice of κ as in (2.28) leads to

$$R_{\text{CFT}_{PW,m=0}} = R_{\text{CFT}_{STU}} + \mathcal{O}\left(\frac{B^4}{T^8}\right). \quad (2.55)$$

2.3.2 $\text{CFT}_{PW,m=\infty}$

The holographic dual to the $\text{CFT}_{PW,m=\infty}$ model can be obtained as a particular decoupling limit $\chi \rightarrow \infty$ of the effective action (2.34). As emphasized originally in [12], the supersymmetric vacuum, and the isotropic thermal equilibrium states of the theory [13, 14] are locally that of the 4 + 1 dimensional conformal plasma. We derive the 5 + 1 dimensional holographic effective action $S_{\text{CFT}_{PW,m=\infty}}$ (trivially) generalizing the arguments of [12].

It is the easiest to start with the $\mathcal{N} = 2^*$ vacuum in a holographic dual, the PW geometry [8]. The IR limit corresponds to $\chi \rightarrow \infty$, thus, introducing a new radial coordinate $u \rightarrow \infty$,

$$e^{2\chi} \simeq 2u, \quad e^{6\alpha} \simeq \frac{2}{3u}, \quad e^A \simeq \left(\frac{2}{3u^4}\right)^{1/3} k, \quad (2.56)$$

the background metric becomes

$$ds_{PW}^2 \simeq \left(\frac{3}{2u^2}\right)^{4/3} \left[4du^2 + \left(\frac{2k}{3}\right)^2 \eta_{\mu\nu} dx^\mu dx^\nu \right]. \quad (2.57)$$

¹⁶It is interesting to investigate whether this \mathbb{Z}_2 symmetry can be spontaneously broken, and if so, what is the role of the magnetic field. This, however, is outside the scope of the current paper.

The parameter $k = 2m$ here is defined as in PW [8, 9]. Introducing [12]

$$e^{4\phi_2} \equiv e^{2(\alpha-\chi)} \simeq \left(\frac{1}{12u^4} \right)^{1/3}, \quad e^{4\phi_1} \equiv e^{6\alpha+2\chi} \simeq \frac{4}{3}, \quad (2.58)$$

the metric (2.57) can be understood as a KK reduction of the locally AdS_6 metric on a compact $x_6 \sim x_6 + L_6$:

$$ds_6^2 = e^{-2\phi_2} ds_{PW}^2 + e^{6\phi_2} dx_6^2 \simeq \frac{3^{3/2}}{2u^2} \left[4du^2 + \left(\frac{2k}{3} \right)^2 \eta_{\mu\nu} dx^\mu dx^\nu + \frac{1}{9} dx_6^2 \right]. \quad (2.59)$$

The metric (2.59) and the scalar ϕ_1 (2.58) is a solution [12] to $d = 6$ $\mathcal{N} = (1, 1)$ $F(4)$ SUGRA [15]

$$S_{F(4)} = \frac{1}{16\pi G_6} \int_{\mathcal{M}_6} d\xi^6 \sqrt{-g_6} \left(R_6 - 4(\partial\phi_1)^2 + e^{-2\phi_1} + e^{2\phi_1} - \frac{1}{16} e^{6\phi_1} \right), \quad (2.60)$$

where, using the PW five-dimensional Newton's constant G_5 ,

$$\frac{L_6}{G_6} = \frac{1}{G_5}. \quad (2.61)$$

Notice that the bulk gauge field in (2.34) can be reinterpreted as a gauge field in the six-dimensional metric (2.59)

$$\underbrace{\sqrt{-g_{PW}} \rho^4 F_{\mu\nu} F^{\mu\nu}}_{\text{in } ds_{PW}^2} = \underbrace{\sqrt{-g_6} e^{2\phi_1} F_{[6]\mu\nu} F_{[6]}^{\mu\nu}}_{\text{in } ds_6^2}, \quad (2.62)$$

leading to

$$S_{\text{CFT}_{PW, m=\infty}} = \frac{1}{16\pi G_6} \int_{\mathcal{M}_6} d\xi^6 \sqrt{-g_6} \left(R_6 - 4(\partial\phi_1)^2 + e^{-2\phi_1} + e^{2\phi_1} - \frac{1}{16} e^{6\phi_1} - 4e^{2\phi_1} F_{[6]\mu\nu} F_{[6]}^{\mu\nu} \right), \quad (2.63)$$

which is precisely the (truncated) effective action of the $F(4)$ gauged supergravity of [17]¹⁷.

Solutions to the gravitational theory (2.63) representing magnetic branes dual to anisotropic magnetized $\mathbb{CFT}_{PW, m=\infty}$ plasma correspond to the following background ansatz:

$$ds_5^2 = -c_1^2 dt^2 + c_2^2 (d\hat{x}^2 + d\hat{y}^2) + c_3^3 (d\hat{z}^2 + d\hat{x}_6) + c_4^2 dr^2, \quad F_{[6]} = B_{[6]} d\hat{x} \wedge d\hat{y}, \quad (2.64)$$

¹⁷The identification is as follows: $A^i = 0$, $B = 0$, $X = e^{-\phi_1}$, $m = \frac{1}{4}$ and $g^2 = \frac{1}{2}$.

where all the metric warp factors c_i as well as the bulk scalar ϕ_1 are functions of the radial coordinate r . The rescaled, *i.e.*, $\hat{\cdot}$ coordinates, are related to PW coordinates x^μ and the KK direction x_6 as follows (compare with (2.59)):

$$\{\hat{t}, \hat{\mathbf{x}}\} \equiv \hat{x}^\mu = \frac{2k}{3}x^\mu, \quad \hat{x}_6 = \frac{1}{3}x_6. \quad (2.65)$$

It is convenient to fix the radial coordinate r and redefine the metric warp factor, the bulk scalar, and the magnetic field as

$$\begin{aligned} c_1 &= \frac{3^{3/4}r}{2^{1/2}} \left(1 - \frac{r_0^5}{r^5}\right)^{1/2} a_1, & c_2 &= \frac{3^{3/4}r}{2^{1/2}} a_2, & c_3 &= \frac{3^{3/4}r}{2^{1/2}}, \\ c_4 &= \frac{3^{3/4}2^{1/2}}{r} \left(1 - \frac{r_0^5}{r^5}\right)^{-1/2} a_4, & B_{[6]} &= \frac{1}{2}r_0^2 \hat{b}, & \phi_1 &= \frac{1}{4} \ln \frac{4}{3} + p. \end{aligned} \quad (2.66)$$

The radial coordinate r changes

$$r \in [r_0, +\infty), \quad (2.67)$$

where r_0 is a location of a regular Schwarzschild horizon, and $r \rightarrow +\infty$ is the asymptotic AdS_6 boundary¹⁸. The bulk scalar field p is dual to a dimension $\Delta = 3$ of the effective five-dimensional boundary conformal theory. Introducing a radial coordinate x as in (2.14) we obtain the following system of ODEs (in a radial coordinate x , $' = \frac{d}{dx}$):

$$\begin{aligned} 0 &= a_1' + \frac{a_1}{36a_2^3x(x^5-1)(2a_2-a_2'x)} \left(18x^2a_2^2(x^5-1)(2a_2^2(p')^2 - (a_2')^2) \right. \\ &\quad \left. + 18xa_2^3(3x^5-8)a_2' - 4a_4^2(27a_2^4 - 8\hat{b}^2x^4)e^{2p} - 9a_2^4(9a_4^2e^{-2p} - e^{6p}a_4^2 - 20) \right), \end{aligned} \quad (2.68)$$

$$\begin{aligned} 0 &= a_4' - \frac{a_4}{36a_2^4x(x^5-1)(2a_2-a_2'x)} \left(18a_2^3x^2(1-x^5)(2a_2^2(p')^2 + 3(a_2')^2) \right. \\ &\quad \left. + x(90a_2^4(x^5-2) + a_4^2(32e^{2p}\hat{b}^2x^4 + 9a_2^4(12e^{2p} + 9e^{-2p} - e^{6p})))a_2' \right. \\ &\quad \left. - 3a_2(a_4^2(32e^{2p}\hat{b}^2x^4 + 3a_2^4(12e^{2p} + 9e^{-2p} - e^{6p})) - 60a_2^4) \right), \end{aligned} \quad (2.69)$$

$$\begin{aligned} 0 &= a_2'' - \frac{(a_2')^2}{a_2} + \frac{1}{36(x^5-1)xa_2^4} \left(a_4^2(32e^{2p}\hat{b}^2x^4 + 9a_2^4(12e^{2p} + 9e^{-2p} - e^{6p})) \right. \\ &\quad \left. + 36a_2^4(x^5-1) \right) a_2' - \frac{32e^{2p}a_4^2\hat{b}^2x^2}{9a_2^3(x^5-1)}, \end{aligned} \quad (2.70)$$

¹⁸ AdS_6 of radius $L_{AdS_6} = 3^{3/4}2^{1/2}$ is a solution with $r_0 = 0$, $\hat{b} = 0$ and $a_1 = a_2 = a_4 \equiv 1$ and $p \equiv 0$.

$$\begin{aligned}
0 = p'' + \frac{1}{36(x^5 - 1)xa_2^4} & \left(a_4^2(32e^{2p}\hat{b}^2x^4 + 9a_2^4(12e^{2p} + 9e^{-2p} - e^{6p})) + 36a_2^4(x^5 - 1) \right) p' \\
& + \frac{a_4^2}{36a_2^4x^2(x^5 - 1)} \left(32e^{2p}\hat{b}^2x^4 - 27a_2^4(4e^{2p} - 3e^{-2p} - e^{6p}) \right).
\end{aligned} \tag{2.71}$$

As before, r_0 is completely scaled out of all the equations of motion. Eqs. (2.68)-(2.71) have to be solved subject to the following asymptotics:

- in the UV, *i.e.*, as $x \rightarrow 0_+$,

$$\begin{aligned}
a_1 = 1 + a_{1,5}x^5 + \mathcal{O}(x^9), \quad a_2 = 1 + \frac{8}{9}\hat{b}^2x^4 + a_{2,5}x^5 + \mathcal{O}(x^7), \\
a_4 = 1 - \frac{4}{3}\hat{b}^2x^4 - (a_{1,5} + 2a_{2,5})x^5 + \mathcal{O}(x^6), \quad p = p_3x^3 + \frac{4}{9}\hat{b}^2x^4 + \mathcal{O}(x^6);
\end{aligned} \tag{2.72}$$

- in the IR, *i.e.*, as $y \equiv 1 - x \rightarrow 0_+$,

$$\begin{aligned}
a_1 = a_{1,h,0} + \mathcal{O}(y), \quad a_2 = a_{2,h,0} + \mathcal{O}(y), \quad p = \ln p_{h,0} + \mathcal{O}(y), \\
a_4 = \frac{30a_{2,h,0}^2 p_{h,0}}{(5p_{h,0}^4(9a_{2,h,0}^4(12 - p_{h,0}^4) + 32\hat{b}^2) + 405a_{2,h,0}^4)^{1/2}} + \mathcal{O}(y).
\end{aligned} \tag{2.73}$$

In total, given \hat{b} , the asymptotic expansions are specified by 6 parameters:

$$\{a_{1,5}, a_{2,5}, p_3, a_{1,h,0}, a_{2,h,0}, p_{h,0}\}, \tag{2.74}$$

which is the correct number of parameters necessary to provide a solution to a system of two second order and two first order equations, $2 \times 2 + 2 \times 1 = 6$. The parameter p_3 corresponds to the expectation value of a dimension $\Delta = 3$ operator of the boundary theory; the other two parameters, $a_{1,5}$ and $a_{2,5}$, determine the expectation value of its stress-energy tensor. Using the standard holographic renormalization we find:

$$\begin{aligned}
\langle T_{[5]\hat{t}\hat{t}} \rangle & \equiv \mathcal{E}_{[5]} = \frac{27r_0^5}{32\pi G_6} (1 - 2a_{1,5} + a_{2,5}), \\
\langle T_{[5]\hat{x}\hat{x}} \rangle = \langle T_{[5]\hat{y}\hat{y}} \rangle & \equiv P_{[5]T} = \frac{27r_0^5}{128\pi G_6} (1 - 2a_{1,5} + 6a_{2,5}), \\
\langle T_{\hat{z}\hat{z}} \rangle = \langle T_{[5]\hat{x}_6\hat{x}_6} \rangle & \equiv P_{[5]L} = \frac{27r_0^5}{128\pi G_6} (1 - 2a_{1,5} - 4a_{2,5}),
\end{aligned} \tag{2.75}$$

for the components of the boundary stress-energy tensor, and

$$s_{[5]} = \frac{27r_0^4 a_{2,h,0}^2}{16G_6}, \quad T_{[5]} = \frac{\sqrt{5}r_0 a_{1,h,0}}{48\pi a_{2,h,0}^2 p_{h,0}} \left[9a_{2,h,0}^4 (9 - p_{h,0}^8 + 12p_{h,0}^4) + 32\hat{b}^2 p_{h,0}^4 \right]^{1/2}, \tag{2.76}$$

for the entropy density and the temperature. Note that,

$$\langle T_{[5] \mu}^{\mu} \rangle = 0. \quad (2.77)$$

There is no renormalization scheme dependence in (2.75), and the trace of the stress-energy tensor vanishes — there is no invariant dimension-five operator that can be constructed only with the magnetic field strength. The (holographic) free energy density is given by the standard relation (2.27). In (2.75)-(2.76) we used the subscript $_{[5]}$ to indicate that the thermodynamic quantities are measured from the perspective of the effective five-dimensional boundary conformal theory; to convert to the four-dimensional perspective, we need to account for (2.65), see also [13],

$$\begin{aligned} \left\{ \mathcal{E}, P_T, P_L \right\} &= \left\{ \mathcal{E}_{[5]}, P_{[5]T}, P_{[5]L} \right\} \times \underbrace{\left(\frac{2k}{3} \right)^4}_{(dt \cdot d\hat{v}ol_3)/(dt \cdot dvol_3)} \times \underbrace{\frac{L_6}{3}}_{\oint d\hat{x}_6}, \\ s &= s_{[5]} \times \underbrace{\left(\frac{2k}{3} \right)^3}_{d\hat{v}ol_3/dvol_3} \times \underbrace{\frac{L_6}{3}}_{\oint d\hat{x}_6}, \quad T = T_{[5]} \times \underbrace{\left(\frac{2k}{3} \right)}_{dt/dt}, \quad b = \hat{b} \times \underbrace{\left(\frac{2k}{3} \right)^2}_{d\hat{x} \wedge d\hat{y}/dx \wedge dy}. \end{aligned} \quad (2.78)$$

As for the other models discussed in this paper, the first law of thermodynamics $d\mathcal{E} = Tds$ (at fixed magnetic field) and the thermodynamic relation $\mathcal{F} = -P_L$ lead to constraints on the numerically obtained parameter set (2.74) (here $' = \frac{d}{db}$):

$$\text{FL} : 0 = \frac{6(2\hat{b}a'_{2,5} - 4\hat{b}a'_{1,5} - 5a_{2,5} + 10a_{1,5} - 5)\sqrt{5}a_{2,h,0}p_{h,0}}{5a_{1,h,0}(32\hat{b}^2p_{h,0}^4 - 9a_{2,h,0}^4(p_{h,0}^8 - 12p_{h,0}^4 - 9))^{1/2}(a'_{2,h,0}\hat{b} - a_{2,h,0})} - 1, \quad (2.79)$$

$$\text{TR} : 0 = \frac{6(1 - 2a_{1,5})p_{h,0}\sqrt{5}}{a_{1,h,0}(32\hat{b}^2p_{h,0}^4 - 9a_{2,h,0}^4(p_{h,0}^8 - 12p_{h,0}^4 - 9))^{1/2}} - 1. \quad (2.80)$$

In appendix B.3 we verified FT and TR in the $\mathbb{CFT}_{PW,m=\infty}$ model to order $\mathcal{O}(\hat{b}^4)$ inclusive; we also present $\mathcal{O}(B^4/T^8)$ results for $R_{\mathbb{CFT}_{PW,m=\infty}}$.

Acknowledgments

Research at Perimeter Institute is supported by the Government of Canada through Industry Canada and by the Province of Ontario through the Ministry of Research & Innovation. This work was further supported by NSERC through the Discovery Grants program.

A Proof of $-P_L = \mathcal{E} - sT$ in holographic magnetized plasma

The proof follows the argument for the universality of the shear viscosity to the entropy density in holographic plasma [22].

Consider a holographic dual to a four dimensional¹⁹ gauge theory in an external magnetic field. We are going to assume that the magnetic field is along the z -direction, as in (2.12). We take the (dimensionally reduced — again, this can be relaxed) holographic background geometry to be

$$ds_5^2 = -c_1^2 dt^2 + c_2^2 (dx^2 + dy^2) + c_3^2 dz^2 + c_4^2 dr^2, \quad c_i = c_i(r). \quad (\text{A.1})$$

At extremality (whether or not the extremal solution is singular or not within the truncation is irrelevant), the Poincare symmetry of the background geometry guarantees that

$$R_{tt} + R_{zz} = 0, \quad (\text{A.2})$$

where $R_{\mu\nu}$ is the Ricci tensor in the orthonormal frame. Clearly, an analogous condition must be satisfied for the full gravitational stress tensor of the matter supporting the geometry

$$T_{tt} + T_{zz} = 0. \quad (\text{A.3})$$

Because turning on the nonextremality will not modify (A.3), we see that (A.2) is valid away from extremality as well. Computing the Ricci tensor for (A.1) reduces (A.2) to

$$0 = R_{tt} + R_{zz} = \frac{1}{c_1 c_2^2 c_3 c_4} \frac{d}{dr} \left[\left(\frac{c_1}{c_3} \right)' \frac{c_2^2 c_3^2}{c_4} \right] \implies \left(\frac{c_1}{c_3} \right)' \frac{c_2^2 c_3^2}{c_4} = \text{const}. \quad (\text{A.4})$$

Explicitly evaluating the ratio of the const in (A.4) in the UV ($r \rightarrow \infty$) and IR ($r \rightarrow r_{horizon}$) we recover

$$0 = \frac{\mathcal{E} + P_L}{sT} - 1, \quad (\text{A.5})$$

for each of the models we study.

We should emphasize that the condition (A.2) can be explicitly verified using the equations of motion in each model studied. The point of the argument above (as the related one in [22]) is that this relation is true based on the symmetries of the problem alone.

¹⁹Generalization to other dimensions is straightforward.

B Conformal models in the limit $T/\sqrt{B} \gg 1$

In holographic models, supersymmetry at extremality typically guarantees that equilibrium isotropic thermodynamics is renormalization scheme independent (compare the $\mathcal{N} = 2^*$ model with the same masses for the bosonic and the fermionic components $m_b^2 = m_f^2$, versus the same model with $m_b^2 \neq m_f^2$ [20]). This is not the case for the holographic magnetized gauge theory plasma in four space-time dimensions, *e.g.*, see [1] for $\mathcal{N} = 4$ SYM. In this appendix we discuss the high temperature anisotropic equilibrium thermodynamics of the conformal (supersymmetric in vacuum) models. For the (locally) four dimensional models (CFT_{diag} , CFT_{STU} and $\text{CFT}_{PW,m=0}$) matching high-temperature equations of state is a natural way to relate renormalization schemes in various theories. In the $\text{CFT}_{PW,m=\infty}$ model, which is locally five dimensional, magnetized thermodynamics is scheme independent.

B.1 CFT_{STU}

The high temperature expansion corresponds to the perturbative expansion in b . In what follows we study anisotropic thermodynamics to order $\mathcal{O}(b^4)$ inclusive. Introducing

$$\begin{aligned} a_1 &= 1 + \sum_{n=1}^{\infty} a_{1,(n)} b^{2n}, & a_2 &= 1 + \sum_{n=1}^{\infty} a_{2,(n)} b^{2n}, & a_4 &= 1 + \sum_{n=1}^{\infty} a_{4,(n)} b^{2n}, \\ \rho &= 1 + \sum_{n=1}^{\infty} \rho_{(n)} b^{2n}, & \nu &= 1 + \sum_{n=1}^{\infty} \nu_{(n)} b^{2n}, \end{aligned} \quad (\text{B.1})$$

so that (see (2.21) and (2.22) for the asymptotics)

$$\begin{aligned} a_{1,2} &= \sum_{n=1}^{\infty} a_{1,2,(n)} b^{2n}, & a_{2,2} &= \sum_{n=1}^{\infty} a_{2,2,(n)} b^{2n}, & r_1 &= \sum_{n=1}^{\infty} r_{1,(n)} b^{2n}, \\ n_1 &= \sum_{n=1}^{\infty} n_{1,(n)} b^{2n}, & a_{1,h,0} &= 1 + \sum_{n=1}^{\infty} a_{1,h,0,(n)} b^{2n}, & a_{2,h,0} &= 1 + \sum_{n=1}^{\infty} a_{2,h,0,(n)} b^{2n}, \\ r_{h,0} &= 1 + \sum_{n=1}^{\infty} r_{h,0,(n)} b^{2n}, & n_{h,0} &= 1 + \sum_{n=1}^{\infty} n_{h,0,(n)} b^{2n}, \end{aligned} \quad (\text{B.2})$$

we find

- at order $n = 1$:

$$0 = a''_{2,(1)} + \frac{x^4 + 3}{x(x^4 - 1)} a'_{2,(1)} - \frac{128x^2}{x^4 - 1}, \quad (\text{B.3})$$

$$0 = a'_{4,(1)} - \frac{4x^4}{3(x^4 - 1)} a'_{2,(1)} + \frac{4(16x^4 + a_{4,(1)})}{x(x^4 - 1)}, \quad (\text{B.4})$$

$$0 = a'_{1,(1)} + \frac{2(x^4 - 3)}{3(x^4 - 1)} a'_{2,(1)} + \frac{4(16x^4 - 3a_{4,(1)})}{3x(x^4 - 1)}, \quad (\text{B.5})$$

$$0 = \rho''_{(1)} + \frac{x^4 + 3}{x(x^4 - 1)} \rho'_{(1)} + \frac{4(16x^4 - 3\rho_{(1)})}{3x^2(x^4 - 1)}, \quad (\text{B.6})$$

$$0 = \nu''_{(1)} + \frac{x^4 + 3}{x(x^4 - 1)} \nu'_{(1)} - \frac{4(16x^4 + \nu_{(1)})}{x^2(x^4 - 1)}; \quad (\text{B.7})$$

■ and at order $n = 2$ (we will not need $\rho_{(2)}$ and $\nu_{(2)}$):

$$0 = a''_{2,(2)} + \frac{x^4 + 3}{x(x^4 - 1)} a'_{2,(2)} - (a'_{2,(1)})^2 + \frac{128x^4 + 24a_{4,(1)}}{3x(x^4 - 1)} a'_{2,(1)} + \frac{512x^2(\nu_{(1)} - \rho_{(1)})}{x^4 - 1} - \frac{128x^2(2a_{4,(1)} - 3a_{2,(1)})}{x^4 - 1}, \quad (\text{B.8})$$

$$0 = a'_{4,(2)} - \frac{4x^4}{3(x^4 - 1)} a'_{2,(2)} + \frac{4a_{4,(2)}}{x(x^4 - 1)} + 2x \left((\rho'_{(1)})^2 + \frac{1}{3}(\nu'_{(1)})^2 \right) + \frac{x(x^4 - 9)}{9(x^4 - 1)} (a'_{2,(1)})^2 - \frac{4(3x^4 a_{4,(1)} - 3a_{2,(1)}x^4 - 32x^4 + 6a_{4,(1)})}{9(x^4 - 1)} a'_{2,(1)} + \frac{8((\nu_{(1)})^2 + 3(\rho_{(1)})^2)}{3x(x^4 - 1)} - \frac{256x^3(\nu_{(1)} - \rho_{(1)})}{x^4 - 1} + \frac{2(96x^4 a_{4,(1)} - 128a_{2,(1)}x^4 + 3(a_{4,(1)})^2)}{x(x^4 - 1)}, \quad (\text{B.9})$$

$$0 = a'_{1,(2)} + \frac{2(x^4 - 3)}{3(x^4 - 1)} a'_{2,(2)} - \frac{4}{x(x^4 - 1)} a_{4,(2)} + \frac{x(x^4 - 9)}{9(x^4 - 1)} (a'_{2,(1)})^2 - \frac{8(\nu_{(1)}^2 + 3\rho_{(1)}^2)}{3x(x^4 - 1)} - \frac{2(3a_{2,(1)}x^4 - 3a_{1,(1)}x^4 - 64x^4 - 9a_{2,(1)} + 12a_{4,(1)} + 9a_{1,(1)})}{9(x^4 - 1)} a'_{2,(1)} - \frac{2}{x(x^4 - 1)} (a_{4,(1)})^2 + 2x \left((\rho'_{(1)})^2 + \frac{1}{3}(\nu'_{(1)})^2 \right) + \frac{4(32x^4 - 3a_{1,(1)})}{3x(x^4 - 1)} a_{4,(1)} + \frac{64x^3(a_{1,(1)} - 4a_{2,(1)})}{3(x^4 - 1)} - \frac{256x^3(\nu_{(1)} - \rho_{(1)})}{3(x^4 - 1)}. \quad (\text{B.10})$$

Eqs. (B.3) and (B.4) can be solved analytically:

$$\begin{aligned}
a_{2,(1)} &= 32 \left(\ln(x) \ln(1+x) - \text{dilog}(x) + \ln(x) \ln(1+x^2) + \text{dilog}(1+x) \right. \\
&\quad \left. + \frac{1}{2} \text{dilog}(1+x^2) \right) + \frac{16}{3} \pi^2, \\
a_{4,(1)} &= \frac{16x^4}{3(x^4-1)} (\pi^2 - 8 \text{dilog}(x) + 8 \ln(x) \ln(x^2+1) + 4 \text{dilog}(x^2+1) + 8 \text{dilog}(1+x) \\
&\quad + 8 \ln(x) \ln(1+x) - 12 \ln(x)),
\end{aligned} \tag{B.11}$$

while the remaining ones have to be solved numerically. We find:

(n)	$a_{1,2,(n)}$	$a_{2,2,(n)}$	$r_{1,(n)}$	$n_{1,(n)}$
(1)	$\frac{16}{3} - \frac{16\pi^2}{9}$	8	$-\frac{4}{3}\pi^2$	$4\pi^2$
(2)	1541.8(0)	-3358.0(0)		

(B.12)

(n)	$a_{1,h,0,(n)}$	$a_{2,h,0,(n)}$	$r_{h,0,(n)}$	$n_{h,0,(n)}$
(1)	-7.2270(2)	$\frac{4}{3}\pi^2$	-9.770(3)	29.310(9)
(2)	1336.5(8)	-2069.9(8)		

(B.13)

An important check on the numerical results are the first law of thermodynamics FL (2.30) and the thermodynamic relation TR (2.32). Given the perturbative expansions (B.2), we can represent

$$\text{FL} = \sum_{n=1}^{\infty} fl_{(n)} b^{2n}, \quad \text{TR} = \sum_{n=1}^{\infty} tr_{(n)} b^{2n}, \tag{B.14}$$

where

■ at order $n = 1$:

$$\begin{aligned}
fl_{(1)} : \quad & 0 = \frac{2}{3} a_{2,h,0,(1)} - 16 - a_{1,h,0,(1)}, \\
tr_{(1)} : \quad & 0 = -2a_{2,h,0,(1)} - \frac{16}{3} - 2a_{1,2,(1)} - a_{1,h,0,(1)};
\end{aligned} \tag{B.15}$$

- and at order $n = 2$:

$$\begin{aligned}
fl_{(2)} : \quad 0 &= \frac{896}{9} - \frac{2}{3}a_{1,h,0,(1)}a_{2,h,0,(1)} + a_{1,h,0,(1)}^2 - 2r_{h,0,(1)}^2 - \frac{2}{3}n_{h,0,(1)}^2 + \frac{19}{9}a_{2,h,0,(1)}^2 \\
&\quad + \frac{64}{3}n_{h,0,(1)} - \frac{64}{3}r_{h,0,(1)} - \frac{4}{3}a_{2,2,(2)} + \frac{32}{3}a_{2,h,0,(1)} + \frac{10}{3}a_{2,h,0,(2)} \\
&\quad + 16a_{1,h,0,(1)} - a_{1,h,0,(2)} + 2a_{1,2,(2)} , \\
tr_{(2)} : \quad 0 &= 2a_{1,h,0,(1)}a_{2,h,0,(1)} + 2a_{1,h,0,(1)}a_{1,2,(1)} + a_{1,h,0,(1)}^2 + 4a_{2,h,0,(1)}a_{1,2,(1)} + \frac{128}{3} \\
&\quad + 3a_{2,h,0,(1)}^2 - 2r_{h,0,(1)}^2 - \frac{2}{3}n_{h,0,(1)}^2 + \frac{32}{3}a_{1,2,(1)} - 2a_{1,2,(2)} + \frac{16}{3}a_{1,h,0,(1)} \\
&\quad - a_{1,h,0,(2)} + 32a_{2,h,0,(1)} - 2a_{2,h,0,(2)} - \frac{64}{3}r_{h,0,(1)} + \frac{64}{3}n_{h,0,(1)} .
\end{aligned} \tag{B.16}$$

Using the results (B.12) and (B.13) (rather, we use more precise values of the parameters reported — obtained from numerics with 40 digit precision) we find

- at order $n = 1$:

$$fl_{(1)} : \quad 0 = -7.7822(6) \times 10^{-15}, \quad tr_{(1)} : \quad 0 = -7.1054(3) \times 10^{-15}; \tag{B.17}$$

- and at order $n = 2$:

$$fl_{(2)} : \quad 0 = -1.9681(5) \times 10^{-6}, \quad tr_{(2)} : \quad 0 = 2.4872(6) \times 10^{-6}. \tag{B.18}$$

Using the perturbative expansion (B.2), it is straightforward to invert the relation between T/\sqrt{B} and b (see (2.25) and (2.15)), and use the results (2.24) with (2.28), along with the analytical values for the parameters (B.12) and (B.13) (and the analytical expression for $a_{1,h,0,(1)}$ obtained from (B.15)) to arrive at

$$\begin{aligned}
R_{\mathbb{CFT}_{STU}} &= 1 - \frac{4B^2}{\pi^4 T^4} \ln \frac{T}{\mu\sqrt{2}} + \left(\frac{\pi^2}{18} + \frac{a_{2,2,(2)}}{512} - \frac{2}{3} + 8 \ln^2 \frac{T}{\mu\sqrt{2}} \right) \frac{B^4}{\pi^8 T^8} + \dots \\
&= 1 - \frac{4B^2}{\pi^4 T^4} \ln \frac{T}{\mu\sqrt{2}} + \left(-6.67694906(1) + 8 \ln^2 \frac{T}{\mu\sqrt{2}} \right) \frac{B^4}{\pi^8 T^8} + \mathcal{O} \left(\frac{B^6}{T^{12}} \ln^3 \frac{T}{\mu} \right) .
\end{aligned} \tag{B.19}$$

It is important to keep in mind that the value $a_{2,2,(2)}$ is sensitive to the matter content of the gravitational dual — set of relevant operators in \mathbb{CFT}_{STU} that develop expectation values in anisotropic thermal equilibrium.

B.2 $\text{CFT}_{PW,m=0}$

The high temperature expansion of the \mathbb{Z}_2 symmetric, *i.e.*, $\chi \equiv 0$ phase, of anisotropic $\text{CFT}_{PW,m=0}$ plasma thermodynamics corresponds to the perturbative expansion in b . In what follows we study anisotropic thermodynamics to order $\mathcal{O}(b^4)$ inclusive. Introducing

$$\begin{aligned} a_1 &= 1 + \sum_{n=1}^{\infty} a_{1,(n)} b^{2n}, & a_2 &= 1 + \sum_{n=1}^{\infty} a_{2,(n)} b^{2n}, & a_4 &= 1 + \sum_{n=1}^{\infty} a_{4,(n)} b^{2n}, \\ \alpha &= \sum_{n=1}^{\infty} \alpha_{(n)} b^{2n}, \end{aligned} \tag{B.20}$$

so that (see (2.41) and (2.42) for the asymptotics)

$$\begin{aligned} a_{2,2,0} &= \sum_{n=1}^{\infty} a_{2,2,0,(n)} b^{2n}, & a_{4,2,0} &= \sum_{n=1}^{\infty} a_{4,2,0,(n)} b^{2n}, & \alpha_{1,0} &= \sum_{n=1}^{\infty} \alpha_{1,0,(n)} b^{2n}, \\ a_{1,h,0} &= 1 + \sum_{n=1}^{\infty} a_{1,h,0,(n)} b^{2n}, & a_{2,h,0} &= 1 + \sum_{n=1}^{\infty} a_{2,h,0,(n)} b^{2n}, \\ r_{h,0} &= 1 + \sum_{n=1}^{\infty} r_{h,0,(n)} b^{2n}, \end{aligned} \tag{B.21}$$

we find

- at order $n = 1$:

$$0 = a''_{2,(1)} + \frac{x^4 + 3}{x(x^4 - 1)} a'_{2,(1)} - \frac{128x^2}{x^4 - 1}, \tag{B.22}$$

$$0 = a'_{4,(1)} - \frac{4x^4}{3(x^4 - 1)} a'_{2,(1)} + \frac{4(16x^4 + a_{4,(1)})}{x(x^4 - 1)}, \tag{B.23}$$

$$0 = a'_{1,(1)} + \frac{2(x^4 - 3)}{3(x^4 - 1)} a'_{2,(1)} + \frac{4(16x^4 - 3a_{4,(1)})}{3x(x^4 - 1)}, \tag{B.24}$$

$$0 = \alpha''_{(1)} + \frac{x^4 + 3}{x(x^4 - 1)} \alpha'_{(1)} + \frac{4(16x^4 - 3\alpha_{(1)})}{3x^2(x^4 - 1)}; \tag{B.25}$$

- and at order $n = 2$ (we will not need $\alpha_{(2)}$):

$$\begin{aligned} 0 &= a''_{2,(2)} + \frac{x^4 + 3}{x(x^4 - 1)} a'_{2,(2)} + \frac{128x^4 + 24a_{4,(1)}}{3x(x^4 - 1)} a'_{2,(1)} - (a'_{2,(1)})^2 \\ &\quad - \frac{128x^2(2a_{4,(1)} + 4\alpha_{(1)} - 3a_{2,(1)})}{x^4 - 1}, \end{aligned} \tag{B.26}$$

$$\begin{aligned}
0 = & a'_{4,(2)} - \frac{4x^4}{3(x^4-1)}a'_{2,(2)} + 2x(\alpha'_{(1)})^2 + \frac{x(x^4-9)}{9(x^4-1)}(a'_{2,(1)})^2 \\
& - \frac{4(x^4(3a_{4,(1)} - 3a_{2,(1)} - 32) + 6a_{4,(1)})}{9(x^4-1)}a'_{2,(1)} + \frac{8\alpha_{(1)}(32x^4 + \alpha_{(1)})}{x(x^4-1)} \\
& + \frac{2(32x^4(3a_{4,(1)} - 4a_{2,(1)}) + 3a_{4,(1)}^2 + 2a_{4,(2)})}{x(x^4-1)}, \tag{B.27}
\end{aligned}$$

$$\begin{aligned}
0 = & a'_{1,(2)} + \frac{2(x^4-3)}{3(x^4-1)}a'_{2,(2)} + \frac{x(x^4-9)}{9(x^4-1)}(a'_{2,(1)})^2 + \frac{2}{9(x^4-1)} \left(x^4(3a_{1,(1)} - 3a_{2,(1)} + 64) \right. \\
& \left. - 9a_{1,(1)} - 12a_{4,(1)} + 9a_{2,(1)} \right) a'_{2,(1)} + 2x(\alpha'_{(1)})^2 - \frac{8\alpha_{(1)}^2}{x(x^4-1)} + \frac{256x^3\alpha_{(1)}}{3(x^4-1)} \\
& - \frac{2}{3x(x^4-1)} \left(6a_{4,(2)} + 32x^4(4a_{2,(1)} - a_{1,(1)}) + 2a_{4,(1)}(-32x^4 + 3a_{1,(1)}) + 3a_{4,(1)}^2 \right). \tag{B.28}
\end{aligned}$$

Eqs. (B.22) and (B.23) can be solved analytically, see (B.11), while the remaining ones have to be solved numerically. We find:

(n)	$a_{2,2,0,(n)}$	$a_{4,2,0,(n)}$	$\alpha_{1,0,(n)}$	$a_{1,h,0,(n)}$	$a_{2,h,0,(n)}$	$r_{h,0,(n)}$
(1)	8	$\frac{16\pi^2}{9}$	$-\frac{4}{3}\pi^2$	-7.2270(2)	$\frac{4}{3}\pi^2$	-9.770(3)
(2)	-1203.9(2)	1064.0(4)		652.34(4)	-863.4(3)	

(B.29)

An important check on the numerical results are the first law of thermodynamics FL (2.51) and the thermodynamic relation TR (2.52). Given the perturbative expansions (B.21), and using the representation (B.14), we find:

■ at order $n = 1$:

$$\begin{aligned}
fl_{(1)} : \quad & 0 = \frac{2}{3}a_{2,h,0,(1)} - 16 - a_{1,h,0,(1)}, \\
tr_{(1)} : \quad & 0 = -2a_{2,h,0,(1)} - 48 - a_{1,h,0,(1)} + 4a_{2,2,0,(1)} + 2a_{4,2,0,(1)}; \tag{B.30}
\end{aligned}$$

■ and at order $n = 2$:

$$\begin{aligned}
fl_{(2)} : 0 &= -\frac{2}{3}a_{2,h,0,(1)}a_{1,h,0,(1)} + \frac{896}{9} + \frac{32}{3}a_{2,h,0,(1)} + \frac{10}{3}a_{2,h,0,(2)} - 2r_{h,0,(1)}^2 + \frac{19}{9}a_{2,h,0,(1)}^2 \\
&+ a_{1,h,0,(1)}^2 - 8\alpha_{1,0,(1)}^2 - a_{1,h,0,(2)} - \frac{16}{3}a_{2,2,0,(2)} - 2a_{4,2,0,(2)} + 16a_{1,h,0,(1)} - \frac{64}{3}r_{h,0,(1)}, \\
tr_{(2)} : 0 &= \frac{2432}{9} - 8a_{2,2,0,(1)}a_{2,h,0,(1)} - 4a_{2,h,0,(1)}a_{4,2,0,(1)} - 4a_{1,h,0,(1)}a_{2,2,0,(1)} \\
&- 2a_{1,h,0,(1)}a_{4,2,0,(1)} + a_{1,h,0,(1)}^2 + 48a_{1,h,0,(1)} - a_{1,h,0,(2)} + \frac{352}{3}a_{2,h,0,(1)} - 2a_{2,h,0,(2)} \\
&+ 2a_{2,h,0,(1)}a_{1,h,0,(1)} + 3a_{2,h,0,(1)}^2 - 2r_{h,0,(1)}^2 + 8\alpha_{1,0,(1)}^2 - \frac{64}{3}r_{h,0,(1)} - \frac{64}{3}a_{2,2,0,(1)} \\
&+ 4a_{2,2,0,(2)} - \frac{32}{3}a_{4,2,0,(1)} + 2a_{4,2,0,(2)}.
\end{aligned} \tag{B.31}$$

Using the results (B.29) (rather, we use more precise values of the parameters reported — obtained from numerics with 40 digit precision) we find

■ at order $n = 1$:

$$fl_{(1)} : \quad 0 = -7.7822(6) \times 10^{-15}, \quad tr_{(1)} : \quad 0 = -2.9555(5) \times 10^{-15}; \tag{B.32}$$

■ and at order $n = 2$:

$$fl_{(2)} : \quad 0 = -1.6451(1) \times 10^{-6}, \quad tr_{(2)} : \quad 0 = 2.2505(2) \times 10^{-6}. \tag{B.33}$$

Using the perturbative expansion (B.21), it is straightforward to invert the relation between T/\sqrt{B} and b (see (2.49) and (2.15)), and use the results (2.47) with (2.28), along with the analytical values for the parameters (B.29), to arrive at

$$\begin{aligned}
R_{\text{CFT}_{PW,m=0}} &= 1 - \frac{4B^2}{\pi^4 T^4} \ln \frac{T}{\mu\sqrt{2}} + \left(\frac{\pi^2}{18} + \frac{a_{2,2,0,(2)}}{512} - \frac{2}{3} + 8 \ln^2 \frac{T}{\mu\sqrt{2}} \right) \frac{B^4}{\pi^8 T^8} + \dots \\
&= 1 - \frac{4B^2}{\pi^4 T^4} \ln \frac{T}{\mu\sqrt{2}} + \left(-2.4697(5) + 8 \ln^2 \frac{T}{\mu\sqrt{2}} \right) \frac{B^4}{\pi^8 T^8} + \mathcal{O} \left(\frac{B^6}{T^{12}} \ln^3 \frac{T}{\mu} \right).
\end{aligned} \tag{B.34}$$

Note that while the first line in (B.34) is equivalent to the corresponding expression in (B.19), the numerical values (compare the second lines) are different: this is related to the fact that the value $a_{2,2,0,(2)}$ in the $\text{CFT}_{PW,m=0}$ dual is “sourced” by a single dimension $\Delta = 2$ operator (the scalar field α in the holographic dual), while the value $a_{2,2,(2)}$ in the CFT_{STU} model is “sourced” by two dimension $\Delta = 2$ operators (the scalar fields ρ and ν in the holographic dual).

B.3 CFT_{PW,m=∞}

The high temperature expansion corresponds to the perturbative expansion in \hat{b} . In what follows we study anisotropic thermodynamics to order $\mathcal{O}(\hat{b}^4)$ inclusive. Introducing

$$\begin{aligned} a_1 &= 1 + \sum_{n=1}^{\infty} a_{1,(n)} \hat{b}^{2n}, & a_2 &= 1 + \sum_{n=1}^{\infty} a_{2,(n)} \hat{b}^{2n}, & a_4 &= 1 + \sum_{n=1}^{\infty} a_{4,(n)} \hat{b}^{2n}, \\ p &= \sum_{n=1}^{\infty} p_{(n)} \hat{b}^{2n}, \end{aligned} \tag{B.35}$$

so that (see (2.21) and (2.22) for the asymptotics)

$$\begin{aligned} a_{1,5} &= \sum_{n=1}^{\infty} a_{1,5,(n)} \hat{b}^{2n}, & a_{2,5} &= \sum_{n=1}^{\infty} a_{2,5,(n)} \hat{b}^{2n}, & p_3 &= \sum_{n=1}^{\infty} p_{3,(n)} \hat{b}^{2n}, \\ a_{1,h,0} &= 1 + \sum_{n=1}^{\infty} a_{1,h,0,(n)} \hat{b}^{2n}, & a_{2,h,0} &= 1 + \sum_{n=1}^{\infty} a_{2,h,0,(n)} \hat{b}^{2n}, \\ p_{h,0} &= 1 + \sum_{n=1}^{\infty} p_{h,0,(n)} \hat{b}^{2n}, \end{aligned} \tag{B.36}$$

we find

- at order $n = 1$:

$$0 = a''_{2,(1)} + \frac{x^5 + 4}{(x^5 - 1)x} a'_{2,(1)} - \frac{32x^2}{9(x^5 - 1)}, \tag{B.37}$$

$$0 = a'_{4,(1)} - \frac{1}{(x^5 - 1)x} \left(\frac{5}{4} a'_{2,(1)} x^6 - 5a_{4,(1)} - \frac{4}{3} x^4 \right), \tag{B.38}$$

$$0 = a'_{1,(1)} + \frac{3x^5 - 8}{4(x^5 - 1)} a'_{2,(1)} + \frac{1}{(x^5 - 1)x} \left(\frac{4}{9} x^4 - 5a_{4,(1)} \right), \tag{B.39}$$

$$0 = p''_{(1)} + \frac{x^5 + 4}{x(x^5 - 1)} p'_{(1)} - \frac{1}{x^2(x^5 - 1)} \left(6p_{(1)} - \frac{8}{9} x^4 \right); \tag{B.40}$$

- and at order $n = 2$ (we will not need $p_{(2)}$):

$$\begin{aligned} 0 &= a''_{2,(2)} + \frac{x^5 + 4}{x(x^5 - 1)} a'_{2,(2)} - (a'_{2,(1)})^2 + \frac{2(4x^4 + 45a_{4,(1)})}{9x(x^5 - 1)} a'_{2,(1)} \\ &\quad + \frac{32x^2}{9(x^5 - 1)} \left(3a_{2,(1)} - 2a_{4,(1)} - 2p_{(1)} \right), \end{aligned} \tag{B.41}$$

$$\begin{aligned}
0 = & a'_{4,(2)} - \frac{1}{x(x^5-1)} \left(\frac{5}{4} a'_{2,(2)} x^6 - 5a_{4,(2)} \right) + \frac{x(x^5-6)}{8(x^5-1)} (a'_{2,(1)})^2 - \frac{1}{36(x^5-1)} \left(\right. \\
& 45a_{4,(1)}x^5 - 45a_{2,(1)}x^5 - 8x^4 + 90a_{4,(1)} \left. \right) a'_{2,(1)} + \frac{x}{2} (p'_{(1)})^2 + \frac{1}{6x(x^5-1)} \left(16x^4 p_{(1)} \right. \\
& \left. + 24x^4 a_{4,(1)} - 32a_{2,(1)}x^4 + 18p_{(1)}^2 + 45a_{4,(1)}^2 \right),
\end{aligned} \tag{B.42}$$

$$\begin{aligned}
0 = & a'_{1,(2)} + \frac{1}{x(x^5-1)} \left(\frac{3}{4} a'_{2,(2)} x^6 - 5a_{4,(2)} - 2a'_{2,(2)}x \right) + \frac{x(x^5-6)}{8(x^5-1)} (a'_{2,(1)})^2 + \frac{x}{2} (p'_{(1)})^2 \\
& + \frac{1}{36(x^5-1)} \left(27a_{1,(1)}x^5 - 27a_{2,(1)}x^5 + 8x^4 - 72a_{1,(1)} - 90a_{4,(1)} + 72a_{2,(1)} \right) a'_{2,(1)} \\
& - \frac{1}{18x(x^5-1)} \left(45a_{4,(1)}^2 - 16x^4 p_{(1)} - 8a_{1,(1)}x^4 - 16x^4 a_{4,(1)} + 32a_{2,(1)}x^4 + 54p_{(1)}^2 \right. \\
& \left. + 90a_{1,(1)}a_{4,(1)} \right).
\end{aligned} \tag{B.43}$$

Eqs. (B.37) and (B.38) can be solved analytically²⁰, while the remaining ones have to be solved numerically. We find:

(n)	$a_{1,5,(n)}$	$a_{2,5,(n)}$	$p_{3,(n)}$	$a_{1,h,0,(n)}$	$a_{2,h,0,(n)}$	$p_{h,0,(n)}$
(1)	-0.25581(6)	$-\frac{32}{45}$	-0.645(2)	-0.12878(5)	0.27576(4)	-0.25155(9)
(2)	0.22327(6)	-0.5489(8)		0.20658(5)	-0.2934(9)	

(B.44)

An important check on the numerical results are the first law of thermodynamics FL (2.79) and the thermodynamic relation TR (2.80). Given the perturbative expansions (B.36), and using the representation (B.14), we find:

- at order $n = 1$:

$$\begin{aligned}
fl_{(1)} : \quad & 0 = -\frac{4}{45} - \frac{2}{5} a_{1,5,(1)} - a_{1,h,0,(1)} + \frac{1}{5} a_{2,5,(1)}, \\
tr_{(1)} : \quad & 0 = -\frac{4}{45} - 2a_{2,h,0,(1)} - 2a_{1,5,(1)} - a_{1,h,0,(1)};
\end{aligned} \tag{B.45}$$

²⁰However, the resulting expressions are too long to be presented here. For the same reason we report only the numerical expression for $a_{2,h,0,(1)}$.

- and at order $n = 2$:

$$\begin{aligned}
fl_{(2)} : \quad 0 &= \frac{8}{675} + \frac{2}{5}a_{1,5,(1)}a_{1,h,0,(1)} - \frac{1}{5}a_{1,h,0,(1)}a_{2,5,(1)} + a_{1,h,0,(1)}^2 + \frac{16}{45}a_{2,h,0,(1)} \\
&\quad + 2a_{2,h,0,(2)} + \frac{4}{45}a_{1,h,0,(1)} - a_{1,h,0,(2)} - \frac{8}{45}p_{h,0,(1)} - \frac{4}{225}a_{2,5,(1)} \\
&\quad - \frac{3}{5}a_{2,5,(2)} + \frac{8}{225}a_{1,5,(1)} + \frac{6}{5}a_{1,5,(2)} - \frac{3}{5}p_{h,0,(1)}^2 + a_{2,h,0,(1)}^2, \\
tr_{(2)} : \quad 0 &= \frac{8}{675} + \frac{8}{15}a_{2,h,0,(1)} - 2a_{2,h,0,(2)} - \frac{8}{45}p_{h,0,(1)} - \frac{3}{5}p_{h,0,(1)}^2 + 3a_{2,h,0,(1)}^2 \\
&\quad + 4a_{2,h,0,(1)}a_{1,5,(1)} + 2a_{2,h,0,(1)}a_{1,h,0,(1)} + 2a_{1,5,(1)}a_{1,h,0,(1)} + a_{1,h,0,(1)}^2 \\
&\quad - 2a_{1,5,(2)} - a_{1,h,0,(2)} + \frac{4}{45}a_{1,h,0,(1)} + \frac{8}{45}a_{1,5,(1)}.
\end{aligned} \tag{B.46}$$

Using results (B.44) (rather, we use more precise values of the parameters reported — obtained from numerics with 40 digit precision) we find

- at order $n = 1$:

$$fl_{(1)} : \quad 0 = 1.8010(4) \times 10^{-12}, \quad tr_{(1)} : \quad 0 = 9.8392(9) \times 10^{-12}; \tag{B.47}$$

- and at order $n = 2$:

$$fl_{(2)} : \quad 0 = -1.0535(2) \times 10^{-12}, \quad tr_{(2)} : \quad 0 = -3.3646(2) \times 10^{-12}. \tag{B.48}$$

Using the perturbative expansion (B.36), it is straightforward to invert the relation between T/\sqrt{B} and \hat{b} (see (2.78)), and arrive at

$$\begin{aligned}
R_{\text{CFT}_{PW,m=\infty}} &= 1 + \frac{3125}{512}a_{2,5,(1)} \frac{B^2}{\pi^4 T^4} + \frac{390625}{4718592} \left(90a_{1,5,(1)}a_{2,5,(1)} + 180a_{1,h,0,(1)}a_{2,5,(1)} \right. \\
&\quad \left. + 180a_{2,5,(1)}^2 + 16a_{2,5,(1)} + 45a_{2,5,(2)} \right) \frac{B^4}{\pi^8 T^8} + \mathcal{O} \left(\frac{B^6}{T^{12}} \right) \\
&= 1 - \frac{625}{144} \frac{B^2}{\pi^4 T^4} + 7.2682(1) \frac{B^4}{\pi^8 T^8} + \mathcal{O} \left(\frac{B^6}{T^{12}} \right).
\end{aligned} \tag{B.49}$$

C FT and TR in a $n\text{CFT}_m$ model

In appendix B we verified the first law of the thermodynamics (FL) and the basic thermodynamic relation $\mathcal{F} = -P_L$ (TR) in various anisotropic magnetized holographic

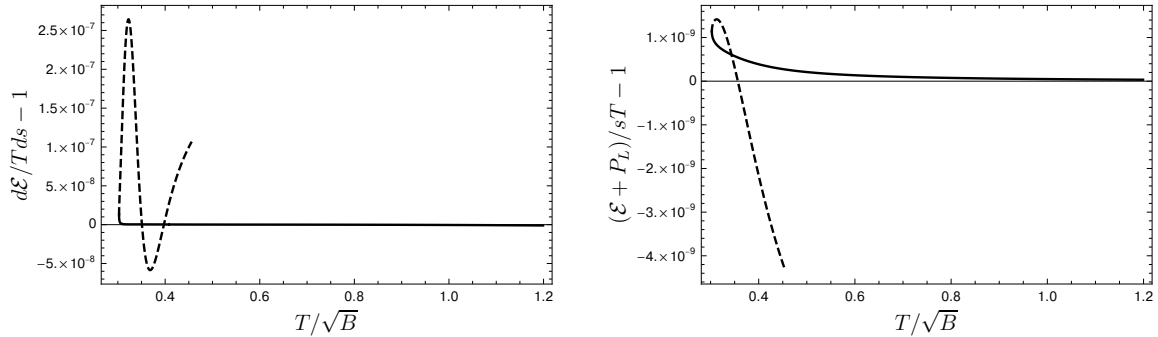


Figure 8: Numerical checks of the first law of thermodynamics $d\mathcal{E} = Tds$ (left panel, fixed B and m) and the basic thermodynamic relation $\mathcal{F} = -P_L$ (right panel) in the $n\text{CFT}_m$ model with $m = \sqrt{2B}$. The dashed parts of the curves indicate thermodynamically unstable branches of the model.

plasma models perturbatively in $\frac{T}{\sqrt{B}} \gg 1$. In fact, we verified both constraints, in all the models considered in the paper, for finite values of $\frac{T}{\sqrt{B}}$. In Fig. 8 we present the checks on these constraints in the $n\text{CFT}_m$ model with $\frac{m}{\sqrt{2B}} = 1$.

References

- [1] G. Endrodi, M. Kaminski, A. Schafer, J. Wu and L. Yaffe, *Universal Magnetoresponse in QCD and $\mathcal{N} = 4$ SYM*, *JHEP* **09** (2018) 070, [1806.09632].
- [2] G. S. Bali, F. Bruckmann, G. Endrodi, F. Gruber and A. Schaefer, *Magnetic field-induced gluonic (inverse) catalysis and pressure (an)isotropy in QCD*, *JHEP* **04** (2013) 130, [1303.1328].
- [3] G. S. Bali, F. Bruckmann, G. Endrodi, S. D. Katz and A. Schaefer, *The QCD equation of state in background magnetic fields*, *JHEP* **08** (2014) 177, [1406.0269].
- [4] E. D’Hoker and P. Kraus, *Magnetic Brane Solutions in AdS*, *JHEP* **10** (2009) 088, [0908.3875].
- [5] J. M. Maldacena, *The Large N limit of superconformal field theories and supergravity*, *Int. J. Theor. Phys.* **38** (1999) 1113–1133, [hep-th/9711200].

- [6] O. Aharony, S. S. Gubser, J. M. Maldacena, H. Ooguri and Y. Oz, *Large N field theories, string theory and gravity*, *Phys. Rept.* **323** (2000) 183–386, [[hep-th/9905111](#)].
- [7] N. Bobev, A. Kundu, K. Pilch and N. P. Warner, *Supersymmetric Charged Clouds in AdS_5* , *JHEP* **03** (2011) 070, [[1005.3552](#)].
- [8] K. Pilch and N. P. Warner, *$N=2$ supersymmetric RG flows and the IIB dilaton*, *Nucl. Phys.* **B594** (2001) 209–228, [[hep-th/0004063](#)].
- [9] A. Buchel, A. W. Peet and J. Polchinski, *Gauge dual and noncommutative extension of an $N=2$ supergravity solution*, *Phys.Rev.* **D63** (2001) 044009, [[hep-th/0008076](#)].
- [10] K. Behrndt, M. Cvetič and W. A. Sabra, *Nonextreme black holes of five-dimensional $N=2$ AdS supergravity*, *Nucl. Phys.* **B553** (1999) 317–332, [[hep-th/9810227](#)].
- [11] M. Cvetič and S. S. Gubser, *Phases of R charged black holes, spinning branes and strongly coupled gauge theories*, *JHEP* **04** (1999) 024, [[hep-th/9902195](#)].
- [12] C. Hoyos, *Higher dimensional conformal field theories in the Coulomb branch*, *Phys. Lett.* **B696** (2011) 145–150, [[1010.4438](#)].
- [13] A. Buchel, *Entanglement entropy of $\mathcal{N} = 2^*$ de Sitter vacuum*, [1904.09968](#).
- [14] A. Buchel, *Bulk viscosity of gauge theory plasma at strong coupling*, *Phys. Lett.* **B663** (2008) 286–289, [[0708.3459](#)].
- [15] L. J. Romans, *The $F(4)$ Gauged Supergravity in Six-dimensions*, *Nucl. Phys.* **B269** (1986) 691.
- [16] M. Cvetič, H. Lu and C. N. Pope, *Gauged six-dimensional supergravity from massive type IIA*, *Phys. Rev. Lett.* **83** (1999) 5226–5229, [[hep-th/9906221](#)].
- [17] K. Chen and M. Gutperle, *Holographic line defects in $F(4)$ gauged supergravity*, *Phys. Rev.* **D100** (2019) 126015, [[1909.11127](#)].
- [18] A. Buchel, M. P. Heller and R. C. Myers, *Equilibration rates in a strongly coupled nonconformal quark-gluon plasma*, *Phys. Rev. Lett.* **114** (2015) 251601, [[1503.07114](#)].

- [19] A. Buchel and C. Pagnutti, *Critical phenomena in $N=2^*$ plasma*, *Phys. Rev.* **D83** (2011) 046004, [1010.3359].
- [20] A. Buchel, S. Deakin, P. Kerner and J. T. Liu, *Thermodynamics of the $N=2^*$ strongly coupled plasma*, *Nucl. Phys.* **B784** (2007) 72–102, [hep-th/0701142].
- [21] K. Skenderis, *Lecture notes on holographic renormalization*, *Class. Quant. Grav.* **19** (2002) 5849–5876, [hep-th/0209067].
- [22] A. Buchel and J. T. Liu, *Universality of the shear viscosity in supergravity*, *Phys. Rev. Lett.* **93** (2004) 090602, [hep-th/0311175].
- [23] V. Balasubramanian and A. Buchel, *On consistent truncations in $N = 2^*$ holography*, *JHEP* **02** (2014) 030, [1311.5044].
- [24] K. Behrndt, A. H. Chamseddine and W. A. Sabra, *BPS black holes in $N=2$ five-dimensional AdS supergravity*, *Phys. Lett.* **B442** (1998) 97–101, [hep-th/9807187].
- [25] O. Aharony, A. Buchel and P. Kerner, *The Black hole in the throat: Thermodynamics of strongly coupled cascading gauge theories*, *Phys. Rev.* **D76** (2007) 086005, [0706.1768].
- [26] A. Buchel, *$N=2^*$ hydrodynamics*, *Nucl. Phys.* **B708** (2005) 451–466, [hep-th/0406200].
- [27] A. Buchel, L. Lehner and R. C. Myers, *Thermal quenches in $N=2^*$ plasmas*, *JHEP* **08** (2012) 049, [1206.6785].